Article

Cell Reports

Reversible Induction of Pain Hypersensitivity following Optogenetic Stimulation of Spinal Astrocytes

Graphical Abstract

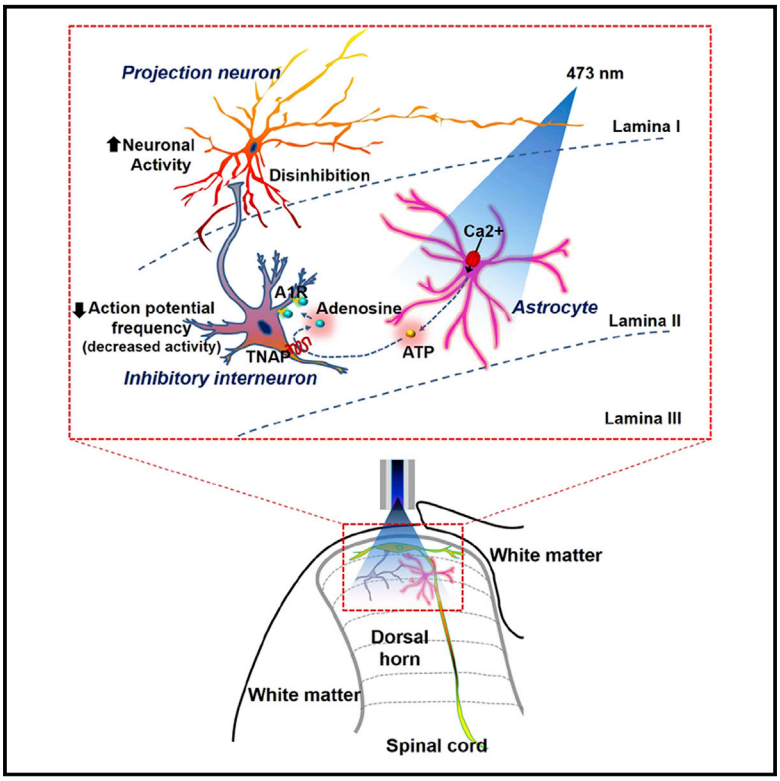

Highlights

- Optogenetics applied to spinal astrocytes in live animals
- Optogenetic stimulation of spinal astrocytes induces pain hypersensitivity
- Spinal astrocytic activation necessary/sufficient for optogenetic pain induction
- Suggests possible basis for therapeutic strategy for chronic pain

Authors

Youngpyo Nam, Jae-Hong Kim, Jong-Heon Kim, ..., Sung-Hun Hwang, Hee-Jung Cho, Kyoungho Suk

Correspondence

ksuk@knu.ac.kr

In Brief

Nam et al. apply optogenetic techniques to spinal cord astrocytes in freely moving rats, finding that spinal astrocytes govern the induction of pain hypersensitivity. The application of microdialysis techniques and electrophysiological studies in conjunction with optogenetics indicate a pivotal role for astrocytes in pain pathogenesis.

Nam et al., 2016, Cell Reports *17*, 3049–3061
December 13, 2016
http://dx.doi.org/10.1016/j.celrep.2016.11.043

Cell Reports
Article

Reversible Induction of Pain Hypersensitivity following Optogenetic Stimulation of Spinal Astrocytes

Youngpyo Nam,[1] Jae-Hong Kim,[1] Jong-Heon Kim,[1] Mithilesh Kumar Jha,[1] Ji Young Jung,[1] Maan-Gee Lee,[1] In-Sun Choi,[2] Il-Sung Jang,[2] Dong Gun Lim,[3] Sung-Hun Hwang,[4] Hee-Jung Cho,[4] and Kyoungho Suk[1,5,*]
[1]Department of Pharmacology, Brain Science & Engineering Institute, BK21 Plus KNU Biomedical Convergence Program, Kyungpook National University School of Medicine, Daegu 41944, Republic of Korea
[2]Department of Pharmacology, School of Dentistry, Kyungpook National University, Daegu 41940, Republic of Korea
[3]Department of Anesthesiology and Pain Medicine, Kyungpook National University School of Medicine, Daegu 41944, Republic of Korea
[4]Department of Anatomy, Kyungpook National University School of Medicine, Daegu 41944, Republic of Korea
[5]Lead Contact
*Correspondence: ksuk@knu.ac.kr
http://dx.doi.org/10.1016/j.celrep.2016.11.043

SUMMARY

While glial activation is an integral part of pain pathogenesis, the existence of a causal relationship between glia and pain processing has yet to be demonstrated in vivo. Here, we have investigated whether the activation of spinal astrocytes could directly evoke pain hypersensitivity in vivo via the use of optogenetic techniques. Optogenetic stimulation of channelrhopdopsin-2 (ChR)-expressing spinal astrocytes induced pain hypersensitivity in a reversible and time-dependent manner, which was accompanied by glial activation, NR1 phosphorylation, ATP release, and the production of proalgesic mediators. Photostimulation of ChR2-expressing astrocytes in culture and spinal slices recapitulated in vivo findings, demonstrating the release of proalgesic mediators and electrophysiological disinhibition of spinal projection neurons. These findings deepen our understanding of the role of astrocytes in pain pathogenesis and provide the scientific basis for an astrocyte-oriented pain treatment.

INTRODUCTION

Chronic pain, induced by either nerve damage (neuropathic pain) or tissue damage (inflammatory pain), is characterized by the hyperactivation of nociceptive neurons in both the peripheral nervous system (peripheral sensitization) and CNS (central sensitization) (Woolf, 2010). The pathogenesis of chronic pain incorporates a series of cellular interactions between CNS-resident cells such as neurons, astrocytes, and microglia. Following peripheral tissue damage, astrocytes in the spinal cord transition to reactive states and participate in the pathogenic mechanisms underlying neuropathic pain (McMahon and Malcangio, 2009). Reactive astrocytes in the dorsal horn of the spinal cord then contribute to the central sensitization by releasing ATP (Duan et al., 2003) and neuromodulators, such as cytokines (interleukin-1β [IL-1β], tumor necrosis factor α [TNF-α], IL-6), chemokines (CCL2) (Gao et al., 2010b), and growth factors (Clark et al., 2013; Guo et al., 2007). However, the existence of a causal relationship between spinal astrocyte activation and pain pathogenesis remains to be determined. Addressing this issue requires the specific and precise modulation of spinal astrocyte activity in their natural physiological setting. Conventionally, electrophysiological and pharmacological approaches have been employed to investigate the functions of neurons and glial cells in the CNS. While such approaches have been employed to great success within this field, they bear several limitations. Primarily, the electrical and pharmacological methods utilized lack the spatiotemporal precision and specificity required to analyze astrocyte-specific events. These circumstances necessitate the formulation of novel in vivo experimental approaches in order to evaluate the exact role of spinal astrocytes in pain pathogenesis.

Optogenetics emerged as an alternative method for stimulating neural activity in living mammalian tissue (Goold and Nicoll, 2010; Nagel et al., 2003) and freely moving animals (Airan et al., 2009; Carter et al., 2010). In recent years, optogenetic tools have been used to explore the role of brain astrocytes in modulating neuronal excitability (Gourine et al., 2010; Sasaki et al., 2012) and to manipulate astrocytes in vivo for the investigation of various disease conditions (Beppu et al., 2014; Sloan and Barres, 2014). Optogenetic techniques have also been utilized in the study of pain processing and pathogenesis (Carr and Zachariou, 2014; Daou et al., 2013; Iyer et al., 2014). However, pain studies that have applied optogenetic strategies in the spinal cord have so far been mostly limited to ex vivo conditions including tissue slices (Wang and Zylka, 2009; Zhang et al., 2014). The optogenetic method has not yet been used to investigate the role of spinal astrocytes in pain in vivo owing to technical difficulties.

RESULTS

Optogenetic Stimulation of Spinal Astrocytes Induces Central Sensitization

To determine the effects of in situ astrocyte activation on pain sensitization, spinal astrocytes were optogenetically stimulated

and behaviors corresponding to pain hypersensitivity were monitored. To achieve this, rats were injected intrathecally with an adenoviral vector expressing the blue-light-sensitive cation channel (channelrhodopsin 2; ChR2 H134R) under the control of the astrocyte-specific GFAP promoter (Ad-ChR2) (Figures S1A and S1B). Spinal cord tissue (cervical, thoracic, and lumbar) was harvested at 10 days post-injection for the histological examination of ChR2 expression. Red fluorescence derived from ChR2 fusion with Katushka1.3 was observed in the lamina I, II, and III regions of the dorsal horn throughout the spinal cord in Ad-ChR2-injected animals (Figure 1A) (higher expression levels in superficial laminae). Immunofluorescence staining with GFAP (an astrocyte marker), Iba-1 (a microglia marker), and NeuN (a neuronal marker) antibodies to characterize the cellular distribution of ChR2 expression was applied to spinal cord sections. As expected, the expression of ChR2 was observed in GFAP+ astrocytes (Figures 1B and 1C), but not microglia or neurons (Figure 1B). For light delivery, an optogenetic cannula was stereotaxically implanted into the vertebra of the lumbar spinal cord and an optogenetic fiber was inserted through the cannula to reach the dorsal horn (Figure 2A). The optogenetic fiber was localized just above dural membrane of the dorsal horn to avoid any potential damage to the spinal cord. The ChR2-expressing spinal astrocytes were exposed to the laser-based illumination through the optogenetic fiber. Before assessing the pain responses, we determined the potential impacts of vertebral cannulation and spinal optogenetic stimulation on motor coordination and reflexive pain behavior. We evaluated the motor functions of each group using the footprint and open-field tests. In addition, acute thermal nociception was analyzed using the tail immersion test (Figure S1C). Subjects within all groups demonstrated similar levels of locomotor ability (Figures S1D and S1E), suggesting that the procedures underlying cannula implantation and optogenetic stimulation did not induce motor deficits, which are prerequisites for the assessment of pain hypersensitivities. Similarly, no significant changes in tail immersion latencies were found between saline- and Ad-ChR2-injected animals following photostimulation (Figure S1F), indicating that reflexive pain behavior was not affected by optogenetic stimulation of spinal astrocytes. These results indicate that the experimental manipulation of spinal cord in this study did not induce any abnormal behaviors.

The laser-based illumination of ChR2-expressing astrocytes through the optogenetic fiber over a 20-min period induced mechanical allodynia and thermal hyperalgesia in the ipsilateral side (Figures 2B–2D). Similar responses were not observed in the unstimulated contralateral side or stimulated ipsilateral side of saline-injected (data not shown) or control adenovirus (Ad-GFP)-injected rats (Figures 2C and 2D). Cannula implantation or laser illumination alone did not influence the hypersensitivity response. In Ad-ChR2-injected rats, pain hypersensitivity responses observed on the stimulated ipsilateral side emerged 1 hr after photostimulation. This was assessed as the maximum response at day 1, which declined thereafter. The optogenetic-stimulation-induced pain hypersensitivity was both transient and reversible. The expression of hypersensitive pain behavior returned to baseline levels after 10 days. Observed pain responses reappeared after the second application of photostimulation and persisted for up to 1 day (Figures 2C and 2D). This indicates that persistent astrocyte activation in the spinal cord is required for chronic pathological pain behavior. Ad-ChR2-injected rats did not exhibit any pain behaviors "during" laser illumination but did show pain behaviors as early as 10 min after photostimulation (data not shown).

Next, we investigated whether the duration of optogenetic stimulation influences the expression of pain hypersensitivity responses. Mechanical and thermal hypersensitivity were evaluated following astrocyte stimulation for 5, 10, or 20 min (Figure 2E). At 1 hr after photostimulation, pain hypersensitivity responses were only detected in the 20-min condition (Figures 2F and 2G). At 1 day after photostimulation, however, these responses were detected in both the 10- and 20-min conditions. Comparatively, the 5-min condition did not induce a significant alteration in pain response over any duration. These findings suggest that the underlying pathogenesis of pain is controlled by the activation duration and status of spinal astrocytes.

Optogenetic Stimulation Induces Glial Activation and Neuronal Excitability in the Spinal Cord Dorsal Horn

Astrocyte activation has been previously associated with central sensitization in various pain-related conditions, including neuropathic pain after peripheral nerve injury (Coyle, 1998) or spinal nerve ligation (Zhuang et al., 2006), and inflammatory pain induced by complete Freund's adjuvant or formalin (Gao et al., 2010a). Therefore, in our optogenetic stimulation model, we evaluated astrocyte activation in the tissue sections of the spinal cord dorsal horn. The immunofluorescence staining of the spinal cord dorsal horn indicated that astrocyte activation was minimally detected in unstimulated Ad-ChR2-injected and stimulated Ad-GFP-injected rats (Figure 3A). However, 1 day after photostimulation in the 20-min condition, a marked increase in fluorescence intensity of GFAP+ astrocytes was observed in the lamina I, II, and III regions within the ipsilateral dorsal horn of Ad-ChR2-injected rats (Figure 3A, upper). In contrast, fluorescence intensity of GFAP+ astrocytes in the contralateral dorsal horn of Ad-ChR2-injected animals did not differ between pre- and post-photostimulation. We counted the number of GFAP+ astrocytes in contralateral and ipsilateral side. The number of GFAP+ cells was not increased by photostimulation (data not shown); instead, there was morphological changes of $GFAP^{+}$ cells in ipsilateral side (photostimulation) compared with contralateral side (no photostimulation). An increased fluorescence intensity in ipsilateral side appears to be due to morphological changes of astrocytes (hypertrophy) after optogenetic stimulation. Activated microglia also participate in the pathological induction of central sensitization by releasing proinflammatory mediators in the spinal cord (Scholz and Woolf, 2007). Subsequently, the role of microglial activation in pain hypersensitivity was assessed following the optogenetic activation of spinal astrocytes. Higher Iba-1-positive microglial activation was observed after photostimulation in the ipsilateral side of the spinal cord dorsal horn in Ad-ChR2-injected rats (Figure 3A, lower), compared with that of the contralateral side or Ad-GFP-injected rats.

To confirm glial activation after optogenetic stimulation, we assessed the activity of mitogen-activated protein kinase (MAPK) in the spinal cord dorsal horn using immunofluorescence

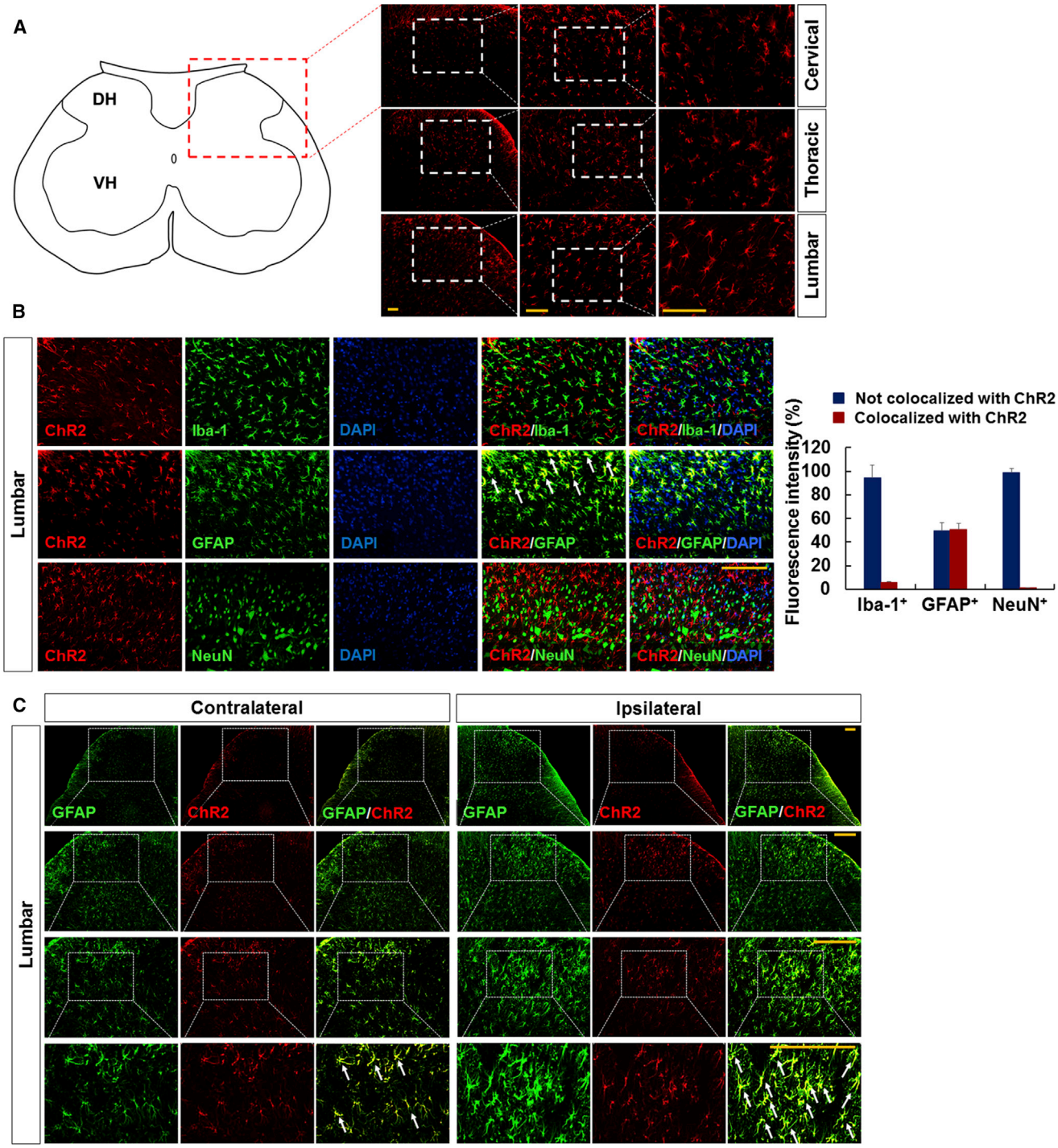

Figure 1. Channelrhodopsin 2-Katushka 1.3 Expression in the Rat Spinal Cord after Ad-ChR2 Infection

(A) ChR2-Katushka 1.3 expression in spinal cords was identified by red fluorescence distributed throughout the dorsal horn of the spinal cord.

(B) The lumbar regions of the spinal cord were subjected to immunofluorescence analysis to localize ChR2 (red) expression in astrocytes (GFAP, green), microglia (Iba-1, green), and neurons (NeuN, green). Nuclei were stained with DAPI (blue). Arrows indicate the co-localization of ChR2 and cell-type-specific markers. Quantification of fluorescence images for GFAP, Iba-1, NeuN, or ChR2-Katushka 1.3 co-localization is shown in the bar graphs.

(C) ChR2-Katushka 1.3 and GFAP expression in lumbar tissues were detected in the spinal ipsilateral (right panel) and contralateral (left panel) side at 1 day after photostimulation. Arrows indicate the co-localization of ChR2 and GFAP. Scale bar, 200 μm. Images are representative of three independent experiments. DH, dorsal horn; VH, ventral horn.

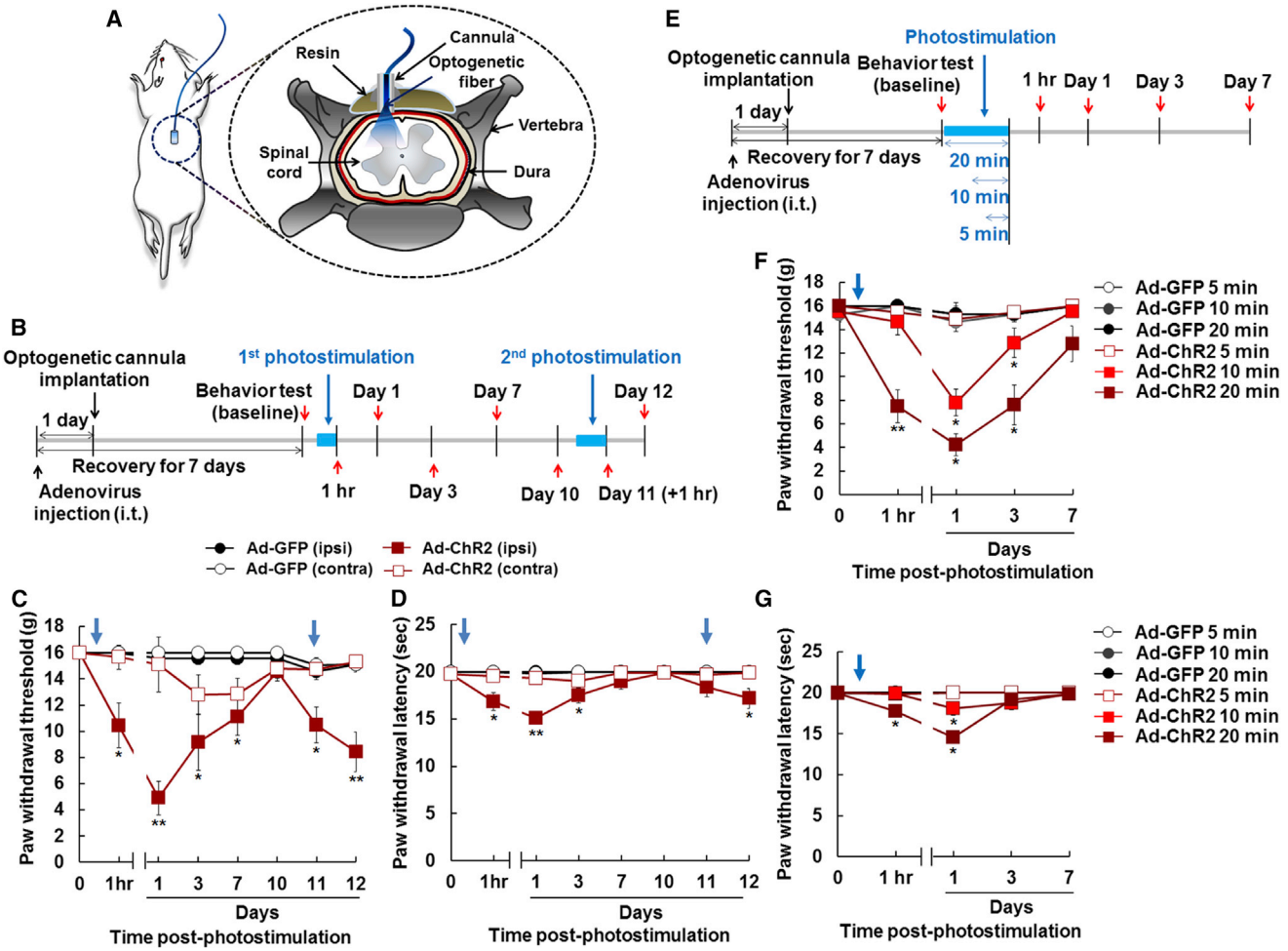

Figure 2. The Optogenetic Stimulation of Spinal Astrocytes Induces Mechanical Allodynia and Thermal Hyperalgesia in Rats

(A) Visual representation of the cannula placement site used to stimulate spinal astrocytes.

(B) Experimental timeline of viral injection, optogenetic cannula implantation, photostimulation, and behavioral analysis. Seven-week-old rats were intrathecally injected with Ad-GFP (n = 6) or Ad-ChR2 (n = 8). On days 7 and 18 post-injection, the first and second sessions of photostimulation were delivered for 20 min to the lamina I and II regions of the spinal cord. Red arrows indicate the time points of behavioral testing.

(C and D) Mechanical (C) and thermal (D) pain hypersensitivity of GFP-expressing or ChR2-expressing rats after first and second photostimulation for 20 min. Blue arrows indicate the time points of photostimulation. Results are expressed as mean ± SEM (n = 6–8). *p < 0.05, **p < 0.01, Ad-GFP ipsi versus Ad-ChR2 ipsi. Data were analyzed using one-way ANOVA with repeated-measurement (paw withdrawal latency) or Mann-Whitney U tests (paw withdrawal threshold).

(E) Experimental timeline of viral injection, cannula implantation, photostimulation, and behavioral analysis for varying durations of photostimulation. Seven days after Ad-GFP (n = 5) or Ad-ChR2 (n = 6) viral injection, photostimulation was delivered for the duration of 5, 10, or 20 min through the optogenetic fiber.

(F and G) Mechanical (F) and thermal (G) pain hypersensitivity of GFP-expressing or ChR2-expressing rats after photostimulation for 5, 10, or 20 min. Blue arrows indicate the time points of photostimulation. Results are expressed as mean ± SEM (n = 5–6).*p < 0.05, **p < 0.01, Ad-GFP ipsi versus Ad-ChR2 ipsi. Data were analyzed using one-way ANOVA with repeated-measurement (paw withdrawal latency) or Mann-Whitney U tests (paw withdrawal threshold).

staining. Alterations in MAPK activity correlate with the activation states of glial cells in diverse chronic pain conditions (Gao and Ji, 2008; White et al., 2011). The upregulation of phospho-p38 and phospho-JNK expression has been reported to co-localize with the activation of spinal microglia (Svensson et al., 2003) and astrocytes (Zhuang et al., 2006), respectively. In the current study, phospho-p38 and phospho-JNK levels increased in the lamina I, II, and III regions of the ipsilateral dorsal horn in Ad-ChR2-injected rats at 1 day after photostimulation (Figure 3B). Conversely, no significant changes in expression level were identified for phospho-p38 or phospho-JNK in saline-injected rats (data not shown) or contralateral dorsal horn in Ad-ChR2-injected rats (Figure 3B). These results indicate that the optogenetic stimulation of astrocytes in the spinal cord induces astrocytic and microglial activation.

The activation of NMDA receptors in the spinal dorsal horn has been established to play a critical role in central sensitization, associated with an increase in neuronal excitability (Woolf and Salter, 2000). Supporting this, previous studies indicate that NMDA receptor phosphorylation is enhanced in spinal dorsal horn neurons in both neuropathic and inflammatory pain models (Gao et al., 2005; Ho et al., 2013). In order to investigate this,

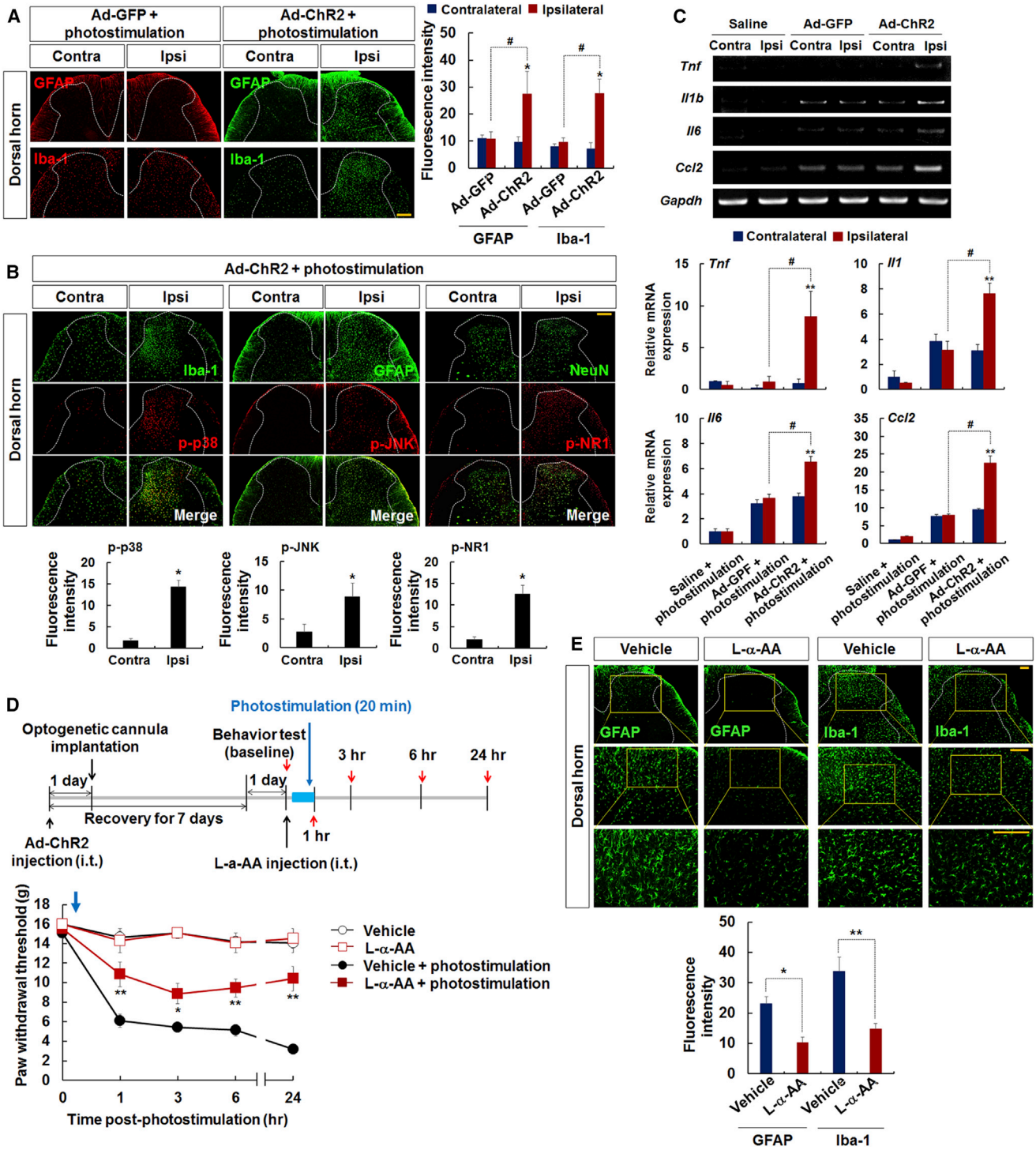

Figure 3. Optogenetic Stimulation Induces Glial Activation and Neuronal Sensitization in the Dorsal Horn of the Spinal Cord

(A) Astrocytes and microglia were identified using anti-GFAP and anti-Iba-1 immunolabeling on day 1 following photostimulation (the peak time point for pain behavior). Dotted white lines indicate the outline of the dorsal horn gray matter. Similar regions of the spinal cord were chosen for all immunofluorescence analyses. The adjacent graph displays the quantification of fluorescence intensity. GFAP, astrocyte-specific marker; Iba-1, microglia-specific marker. Scale bar, 200 μm. Results are expressed as mean ± SEM (n = 4). *p < 0.05 versus contralateral side; #p < 0.05 between the indicated groups (one-way ANOVA with Bonferroni's post hoc test).

(legend continued on next page)

phospho-NR1 expression in the dorsal horn was evaluated after optogenetic stimulation. Following photostimulation in the 20-min condition, p-NR1 Ser896 immunoreactivity was markedly upregulated in the lamina I, II, and III regions of the ipsilateral dorsal horn, compared with the contralateral side (Figure 3B) or saline-injected animals (data not shown). Furthermore, c-Fos expression also increased in the ipsilateral dorsal horn following photostimulation (Figure S2). These results suggest that the optogenetic stimulation of astrocytes heightens neuronal excitability in the spinal cord.

Cytokines and chemokines are key participants in the induction and maintenance of pain pathogenesis. The activation of astrocytes and microglia has been widely acknowledged to contribute to pain pathogenesis via the release of proinflammatory and proalgesic mediators, including TNF-α, IL-1β, IL-6, and CCL2 (Clark et al., 2013). To determine whether the optogenetic stimulation of astrocytes affects the expression of proinflammatory genes in the spinal cord, both the contralateral and ipsilateral sides of the spinal cord were harvested for saline-injected, Ad-GFP-injected, and Ad-ChR2-injected rats at 1 day after photostimulation. The expression of *Tnf*, *Il1b*, *Il6*, and *Ccl2* mRNA was significantly enhanced in the ipsilateral side of ChR2-injected rats, compared with that of saline-injected and Ad-GFP-injected rats (Figure 3C). These results indicate that the optogenetic stimulation of astrocytes enhances the expression of proinflammatory cytokines and chemokines in the spinal cord.

Inhibition of astrocyte activation by L-α-AA (astroglial toxin) or fluorocitrate (astrocytic metabolic inhibitor) has been previously reported to reduce pathological pain responses (Jiang et al., 2016; Sung et al., 2012), and we confirmed that intrathecal administration of L-α-AA was able to attenuate the peripheral nerve-injury-induced neuropathic pain (data not shown). To determine whether astrocyte activation is necessary to induce pain hypersensitivity after optogenetic stimulation, we intrathecally injected L-α-AA or fluorocitrate to rats before photostimulation of spinal astrocytes. After photostimulation for 20 min, L-α-AA-injected rats showed a significantly attenuated mechanical allodynia (Figure 3D) and thermal hyperalgesia (data not shown) compared with vehicle-injected animals. In addition, fluorocitrate-injected rats similarly exhibited less pain response compared with control animals (data not shown). We evaluated glial activation in the tissue sections of the spinal cord dorsal horn by the immunofluorescence staining. At 1 day after photostimulation in the 20-min condition, astrocytes and microglial activation was significantly higher in ipsilateral side of vehicle-injected rats than L-α-AA-injected animals (Figure 3E). These results support a crucial role for astrocytic activation in the optogenetic induction of pain behavior; spinal astrocyte activation is sufficient and necessary for the optogenetic induction of pain.

Microglial Activation Is Causally Implicated in Pain Hypersensitivity following Optogenetic Stimulation

As discussed above, activated microglia release a variety of proinflammatory cytokines and chemokines to augment nociceptive signal transmission or central sensitization in the spinal cord (Marchand et al., 2005). Since a large degree of microglial activation was observed in the spinal dorsal horn after optogenetic stimulation (Figure 3), we sought to further examine their role by depleting microglia in vivo. This was achieved via administration of clodronate (Figure S3A). Clodronate or saline was administered daily via the intracerebroventricular (i.c.v.) route for 4 days prior to photostimulation. The administration of clodronate successfully depleted spinal dorsal horn microglia, as demonstrated via staining with Iba-1, but did not have significant effects on astrocytes (Figures S3B and S3C). Clodronate-induced microglial depletion was recovered to control levels after 14–30 days (Figure S3B). Pain hypersensitivity induced by photostimulation was significantly attenuated by microglial depletion at 1 day after photostimulation (Figures S3D and S3E). These findings indicate that the activation of microglia features a causal relationship with pain hypersensitivity following the optogenetic stimulation of astrocytes in the spinal cord.

Optogenetic Stimulation of Astrocytes Induces the Release of ATP and Proinflammatory Mediators in the Dorsal Horn of the Spinal Cord

Purinergic receptors, such as the P2X7 receptor, have been associated with the release of proinflammatory mediators, particularly those that contribute to pain processing and transmission (Duan et al., 2003). Accordingly, ATP induces the activation of purinergic receptors expressed on neurons, microglia, and astrocytes in the spinal cord (Illes et al., 2012; Tsuda et al., 2003, 2007). To determine whether optogenetic stimulation triggers the release of ATP in the dorsal horn, interstitial fluid from the spinal cord was obtained using microdialysis (Figures 4A and 4B). Microdialysis samples were collected from the spinal cord 2 hr prior to and after the photostimulation of Ad-ChR2-injected rats. Following photostimulation for 20 min, the ATP concentration in the dialysate was increased by up to 2.5-fold (Figure 4C). Such results indicate that stimulated astrocytes induce the release of ATP in the dorsal horn of the spinal cord, concurrent with the induction of pain hypersensitivity.

(B) Expression levels of p-JNK, p-p38, and p-NR1 were assessed using specific antibodies to indicate levels of astrocytic, microglial, and neuronal sensitization. Dotted white lines indicate the outline of the dorsal horn gray matter. Scale bar, 200 μm. The graph displays quantification of fluorescence intensity. Results are expressed as mean ± SEM (n = 4). *p < 0.05 versus contra (Student's t test).

(C) On day 1 following photostimulation, total mRNA was extracted from the lumbar spinal cord of each group and underwent RT-PCR to assess the expression levels of *Tnf*, *Il1b, Il6,* and *Ccl2. Gapdh* was used as an internal control. The graph displays quantitative results normalized to *Gapdh*; results are expressed as mean ± SEM (n = 4). *p < 0.05, **p < 0.01 versus contralateral side; #p < 0.05 between the indicated groups (one-way ANOVA with Bonferroni's post hoc test).

(D) L-α-AA (10 nM) or vehicle was injected intrathecally, and then spinal astrocytes were photostimulated for 20 min (indicated by blue arrows) by delivering blue laser (473 nm) through optogenetic fiber. Red arrows indicate the time points of behavioral assessment. Results are expressed as mean ± SEM (n = 6). *p < 0.05, **p < 0.01, vehicle + photostimulation versus L-α-AA + photostimulation. Data were analyzed using Mann-Whitney U tests.

(E) Frozen sections of lumbar spinal cords taken from vehicle-injected or L-α-AA-injected rats at day 1 after photostimulation were stained with anti-GFAP and anti-Iba-1 antibodies. Dotted white lines indicate the outline of the dorsal horn gray matter. The graph displays quantification of fluorescence intensity. Results are expressed as mean ± SD (n = 3). *p < 0.05 versus vehicle (Student's t test).

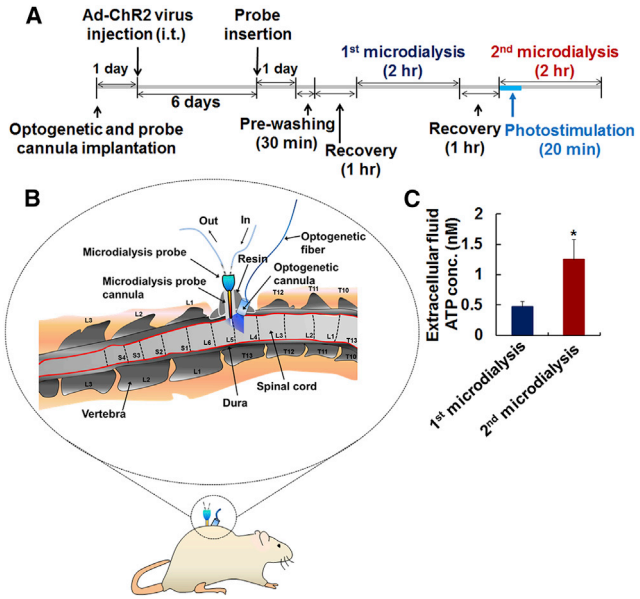

Figure 4. ATP Release Is Increased following Photostimulation of ChR2-Expressing Astrocytes in the Spinal Cord

(A) Experimental timeline of virus injection, insertion of optogenetic cannula and dialysis probe, photostimulation, and microdialysis. The microdialysis probe was inserted into the dorsal horn 24 hr prior to the start of the microdialysis and perfused for 30 min (pre-washing) with artificial cerebrospinal fluid. This was completed 1 hr prior to microdialysis to avoid the confounding effects of tissue injury caused by probe insertion. Microdialysis was performed at a flow rate of 0.5 μl/min for 2 hr before and after photostimulation for 20 min.

(B) Two cannulas (one for the optogenetic fiber, and the other for the microdialysis probe) were implanted stereotaxically into the lumbar spinal cord. The cannula for photostimulation was inserted obliquely, whereas the cannula for the microdialysis probe was inserted perpendicularly into the dorsal horn of the spinal cord.

(C) Extracellular ATP concentration in the dialysate was measured using a bioluminescence assay prior to and after photostimulation. The results are expressed as mean ± SEM (n = 6). *p < 0.05, first microdialysis versus second microdialysis (Student's t test).

Additional in vitro experiments using cultured astrocytes provided evidence to support these results. Primary astrocyte cultures were infected with Ad-GFP or Ad-ChR2 (Figure S4A), and the concentration of ATP in the culture media was measured immediately after photostimulation (Figures 5A and 5B). Photostimulation for the 10 or 20 min, but not the 5-min condition, induced ATP release in vitro (Figure 5C). However, when culture media were collected at 6 hr after photostimulation, no significant increase of ATP release was found in any conditions tested (Figure S4C). The production of proinflammatory mediators in vivo following the optogenetic stimulation of spinal astrocytes was also confirmed using cultured astrocytes. LED stimulation of cultured astrocytes induced the mRNA expression of *Tnf*, *Il1b*, *Il6*, and *Ccl2* (Figure 5D). TNF-α protein production was also significantly increased in the astrocyte culture media following LED stimulation (Figure 5E). We also measured astrocytic intracellular calcium level and membrane current using calcium indicator Fluo-4 or whole-cell patch-clamp to confirm the astrocyte activation following optogenetic stimulation. ChR2-expressing astrocytes showed an increased intracellular Ca^{2+} level ($[Ca^{2+}]_i$) following photostimulation (data not shown). Photostimulation of ChR2-expressing astrocytes also induced inwardly directed currents (Figure S4B). Furthermore, photostimulation for any duration failed to induce a significant degree of cytotoxicity in astrocyte cultures (Figure 5F). These results demonstrate that the photostimulation of ChR2-expressing astrocytes induces ATP release and the expression of proinflammatory mediators.

Optogenetic Stimulation of Astrocytes in Spinal Cord Slices Inhibits GABAergic Inhibitory Interneuron Activities

We examined whether the photoactivation of astrocytic ChR2 can affect the excitability of spinal dorsal horn neurons. In organotypic slice cultures, ChR2 was expressed in astrocytes (Figure S5A), and membrane voltage was measured from dorsal horn neurons using a whole-cell patch-clamp technique. In all dorsal horn neurons tested (n = 7), the tonic firing pattern was observed in response to the depolarizing current injection (Figure 6A). In these neurons, photostimulation decreased action potential frequency to 39.6% ± 9.2% of the control (2.53 ± 0.96 Hz for the control and 1.28 ± 0.70 Hz for the 473-nm condition, n = 8, $p < 0.01$) (Figures 6B and 6C) and induced a hyperpolarization (−57.3 ± 1.2 mV for the control and −62.7 ± 0.9 mV for the 473-nm condition, n = 7, $p < 0.01$) (Figures 6B and 6D, left). The photostimulation-induced increase in action potential frequency was completely blocked by 1 μM dipropylcyclopentylxanthine (DPCPX), a selective adenosine A1 receptor antagonist (98.0% ± 8.0% of the DPCPX condition, n = 8, p = 0.63) (Figures 6B and 6C). In addition, The photostimulation-induced membrane hyperpolarization was completely blocked by 1 μM DPCPX (−57.5 ± 1.1 mV for the DPCPX condition and −57.6 ± 1.3 mV for the 473-nm condition in the presence of DPCPX, n = 7, p = 0.59) (Figures 6B and 6D, right). We also determined whether the recorded neurons are excitatory or inhibitory using a single-cell RT-PCR technique. In all dorsal horn neurons tested (n = 7), transcript for vesicular inhibitory amino acid transporter (VIAAT; inhibitory neuronal marker), but not vesicular glutamate transporter 2 (VGluT2; excitatory neuronal marker), was detected (Figure 6E, left). Lack of detection of transcript for VGluT2 was not due to an inadequate PCR primer used, because transcript for VGluT2 was clearly detected in excitatory neurons from the dorsal horn (Figure 6E, middle) and the entire dorsal horn region (Figure 6E, right). Effects of optogenetic stimulation of spinal astrocytes on the excitation of the projection neurons were determined by immunofluorescence staining with neurokinin-1 receptor (NK1R; a projection neuron marker) and c-Fos antibodies. After photostimulation for 20 min, c-Fos expression was markedly increased in projection neurons of spinal lamina I region in the ipsilateral side compared with contralateral side (Figure S5D). As for the influence of photostimulation on membrane properties of adjacent neurons, we tested whether photostimulation affects the passive membrane properties of dorsal horn neurons in the presence of DPCPX. We found that photostimulation did not change the input resistance or the action potential threshold examined by rheobase currents (Figures S5E and S5F). These data suggest that photostimulation does not affect the membrane properties of dorsal horn neurons. Also, it should

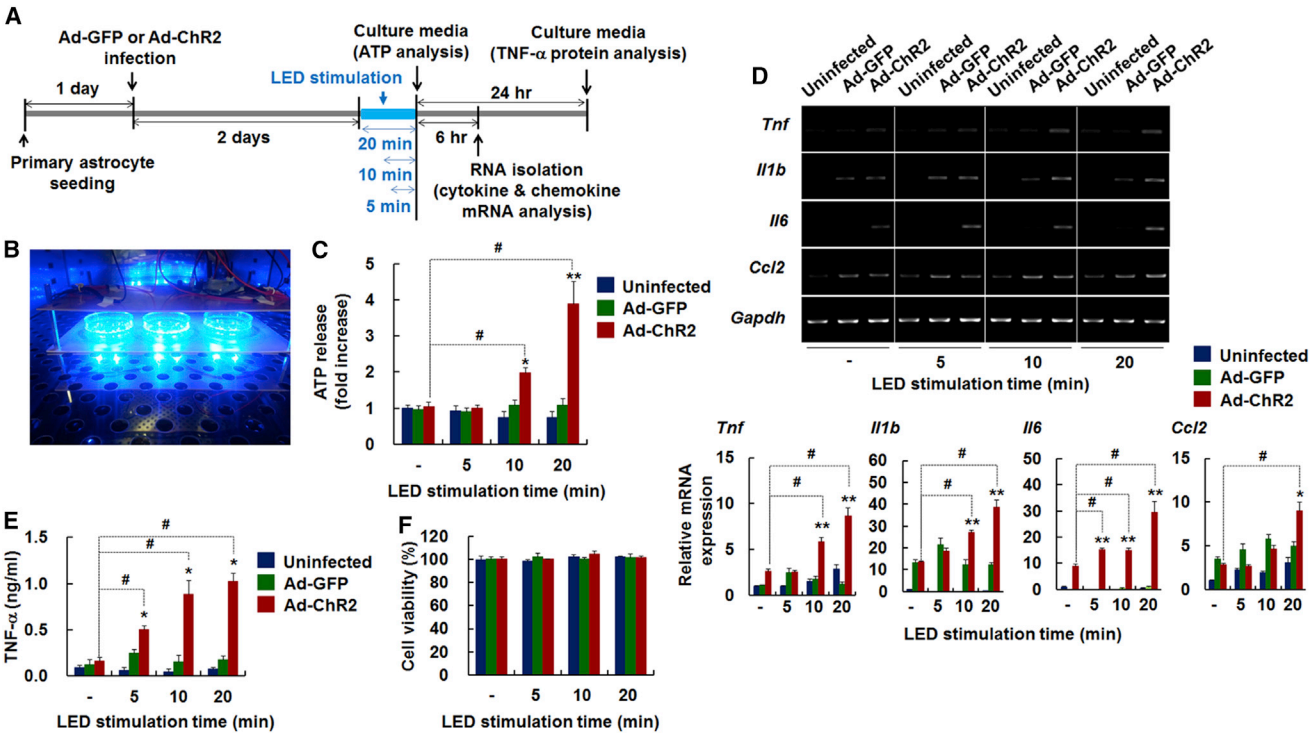

Figure 5. Photostimulated ChR2-Expressing Astrocytes in Culture Demonstrate Elevated Release of ATP and Proinflammatory Mediators

(A) Experimental timeline of virus infection, LED stimulation, and ATP or RNA analysis.

(B) Image displaying LED stimulation of astrocytes in culture.

(C) Primary astrocyte cultures were illuminated using the LED device for 5–20 min, and culture media were collected immediately after stimulation. ATP release from astrocytes infected with Ad-GFP or Ad-ChR2 was measured using a bioluminescence assay.

(D) Total RNA was isolated following 6 hr of LED stimulation. Levels of *Tnf, Il1b*, *Il6*, and *Ccl2* mRNA were determined by RT-PCR (upper). Data were normalized to *Gapdh*, and the results are expressed as mean ± SD (n = 4) in the graph (lower). *$p < 0.05$, **$p < 0.01$ versus uninfected astrocytes; $^{\#}p < 0.05$ between the indicated groups (one-way ANOVA with Bonferroni's post hoc test).

(E) TNF-α protein release from astrocytes was measured by ELISA after 24 hr of LED stimulation.

(F) Viability of astrocytes following viral infection and LED stimulation was assessed using an MTT assay after 24 hr of LED stimulation. Results are expressed as mean ± SD (n = 4). *$p < 0.05$ versus uninfected; $^{\#}p < 0.05$ between the indicated groups (one-way ANOVA with Bonferroni's post hoc test).

be noted that photostimulation induced inwardly directed membrane currents in astrocytes (Figures S5B and S5C), but not in dorsal horn neurons. Given that optogenetic stimulation decreased the excitability of inhibitory interneurons within the dorsal horn region, and extracellular ATP can be easily hydrolyzed by several enzymes within the dorsal horn region (Choi et al., 2015; Street et al., 2013), we next investigated the expression of tissue non-specific alkaline phosphatase (TNAP), which hydrolyses extracellular ATP. To examine the TNAP expression in GAD67+ inhibitory neurons, we have conducted triple immunofluorescence staining using anti-NK1R, anti-TNAP, and anti-GAD67 antibodies. Our data indicate that TNAP is co-localized with GAD67+ inhibitory interneurons in lamina II region, but not NK1R+ projection neurons (Figure S5G). These results indicated that ATP released from astrocytes during photostimulation of astrocytic ChR2 is likely to be converted into adenosine and disinhibit spinal projection neurons in an A1-receptor-dependent manner. Next, we investigated whether the DPCPX administration influences the pain hypersensitivity responses after optogenetic stimulation. Animals were intrathecally injected with DPCPX before optogenetic stimulation of spinal astrocytes (Figure 6F). After photostimulation for 20 min, DPCPX-injected rat showed decreased mechanical allodynia compared with vehicle-injected rats (Figure 6G). These results suggest that astrocytic ATP released by optogenetic stimulation induces pain hypersensitivity through adenosine receptors.

Optogenetic Stimulation of Spinal Astrocytes Enhances Neuropathic Pain Responses

The activation of spinal astrocytes has been observed in various models of neuropathic pain, including the spared nerve and chronic constrictive injury models. According to previous studies, microglial activation precedes astrocyte activation, suggesting that glial activation is important for the induction and maintenance of pain pathogenesis. In some reports, however, astrocyte activation was observed prior to that of microglia, implying that activated astrocytes might initiate the pain response (Gwak et al., 2012; Honore et al., 2000; Zhang et al., 2012). The time sequence of microglial and astrocyte activation is also a controversial subject, as demonstrated in a previous study concerning patients with chronic pain (Shi et al., 2012).

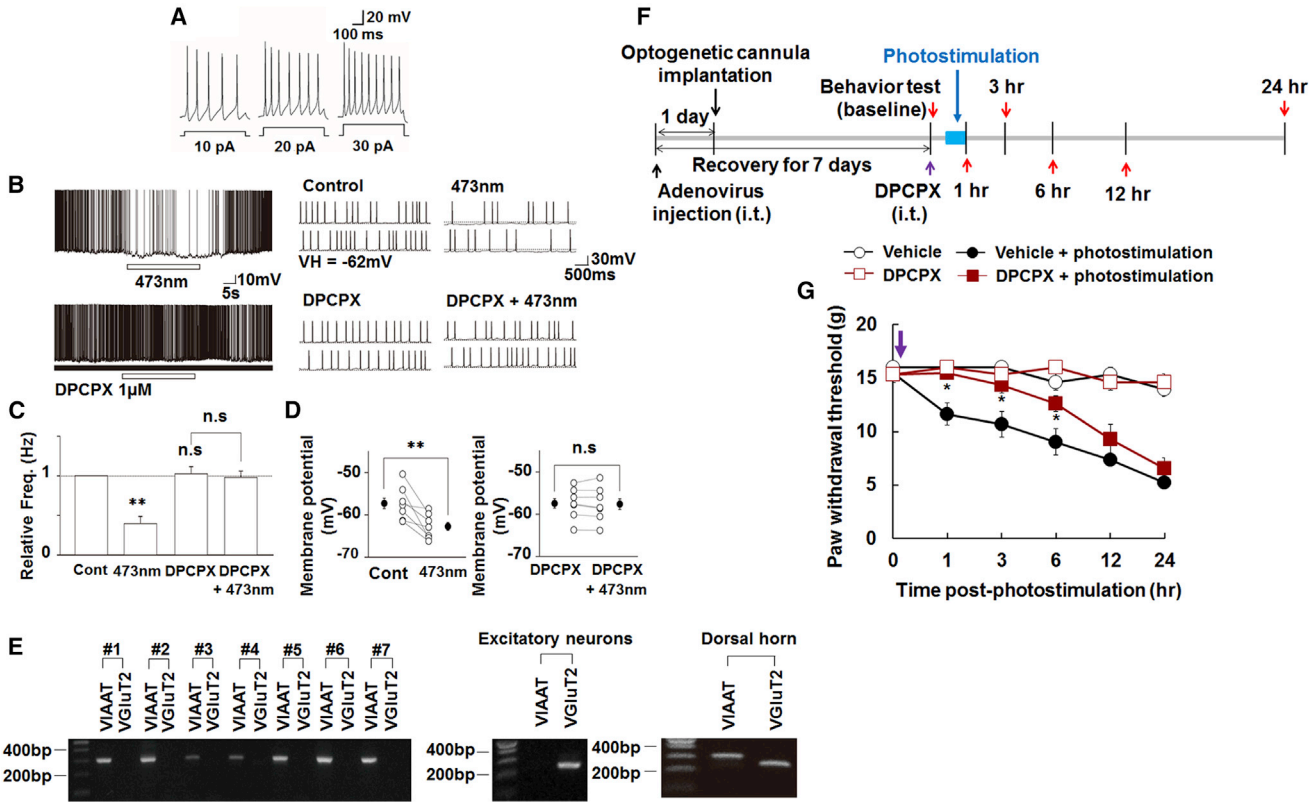

Figure 6. Effects of Photostimulation of ChR2-Expressing Astrocytes on the Excitability of Spinal Dorsal Horn Neurons

(A) Typical trace of voltage response during the depolarizing current injection.

(B) Typical traces of voltage responses before, during and after photostimulation (473 nm, 500-ms duration, 1 Hz) in the absence (B, upper left) and presence (B, lower left) of 1 μM DPCPX, a selective adenosine A1 receptor antagonist. Typical traces of voltage responses shown in (B) with an expanded timescale (B), right).

(C) Photostimulation-induced changes of action potential frequency in dorsal horn neurons. Each column represents the mean and SEM from seven experiments. **$p < 0.01$; n.s, not significant.

(D) Photostimulation-induced changes in membrane potentials in the absence (left) and presence (right) of 1 μM DPCPX. Open circles and connected lines represent the individual results, whereas closed circles and error bars indicate the mean and SEM from seven experiments. **$p < 0.01$, n.s; not significant.

(E) Single-cell RT-PCR analysis revealed the expression of transcript for VIAAT (301 bp), but not VGluT2 (259 bp) (left). Similar results were obtained from seven independent experiments. cDNA samples from excitatory neurons of the dorsal horn (middle) and entire dorsal horn region (right) were used as a control.

(F) Experimental timeline of virus injection, optogenetic cannula implantation, DPCPX injection, photostimulation, and behavioral analysis. Seven days post-viral injection, animals were injected intrathecally with DPCPX (5 μg) or vehicle (as indicated by purple arrows). Rats then underwent photostimulation for 20 min (indicated by blue arrows), followed by behavioral testing (indicated by red arrows).

(G) Injection of DPCPX decreased mechanical pain responses after photostimulation. The results are expressed as mean ± SEM (n = 5). *$p < 0.05$, vehicle + photostimulation versus DPCPX + photostimulation. Data were analyzed using Mann-Whitney U tests (paw withdrawal threshold).

Having demonstrated that the optogenetic activation of spinal astrocytes alone elicited the induction of pain hypersensitivity (Figure 2), we next investigated the involvement of spinal astrocytes in peripheral nerve-injury-induced neuropathic pain behavior. In the spared nerve injury (SNI) neuropathic pain model, astrocyte activation is usually observed at 8 days post-surgery, whereas microglial activation is often identified at approximately 4 days after (data not shown). Therefore, in the next set of experiments, the optogenetic stimulation of astrocytes occurred on the first day post-surgery, earlier than the microglial activation phase to determine the role of astrocytes in the early stages of neuropathic pain (Figure 7A). The forced activation of astrocytes using photostimulation for 10 min produced an intensifying effect on the pain hypersensitivity induced by peripheral nerve injury (Figure 7B). We evaluated microglial activation in the tissue sections of the spinal cord dorsal horn using immunofluorescence staining with Iba-1 and phospho-p38 antibodies. At 1 day after photostimulation, microglial activation was higher in ipsilateral side of SNI + photostimulated rats compared with SNI surgery alone (Figure 7C). These results indicate that astrocyte activation might play a critical role in the initiation phase of chronic pain.

Based on the optogenetics experiment data, we determined whether early administration of astrocytes inhibitor affects SNI-induced pain development. Animals were injected with L-α-AA or vehicle intrathecally immediately after SNI surgery (Figure S6A). Surprisingly, early administration of L-α-AA attenuated microglial activation as well as mechanical allodynia (Figures S6B and S6C). In addition, we investigated the mRNA expression associated with microglial activation under these conditions

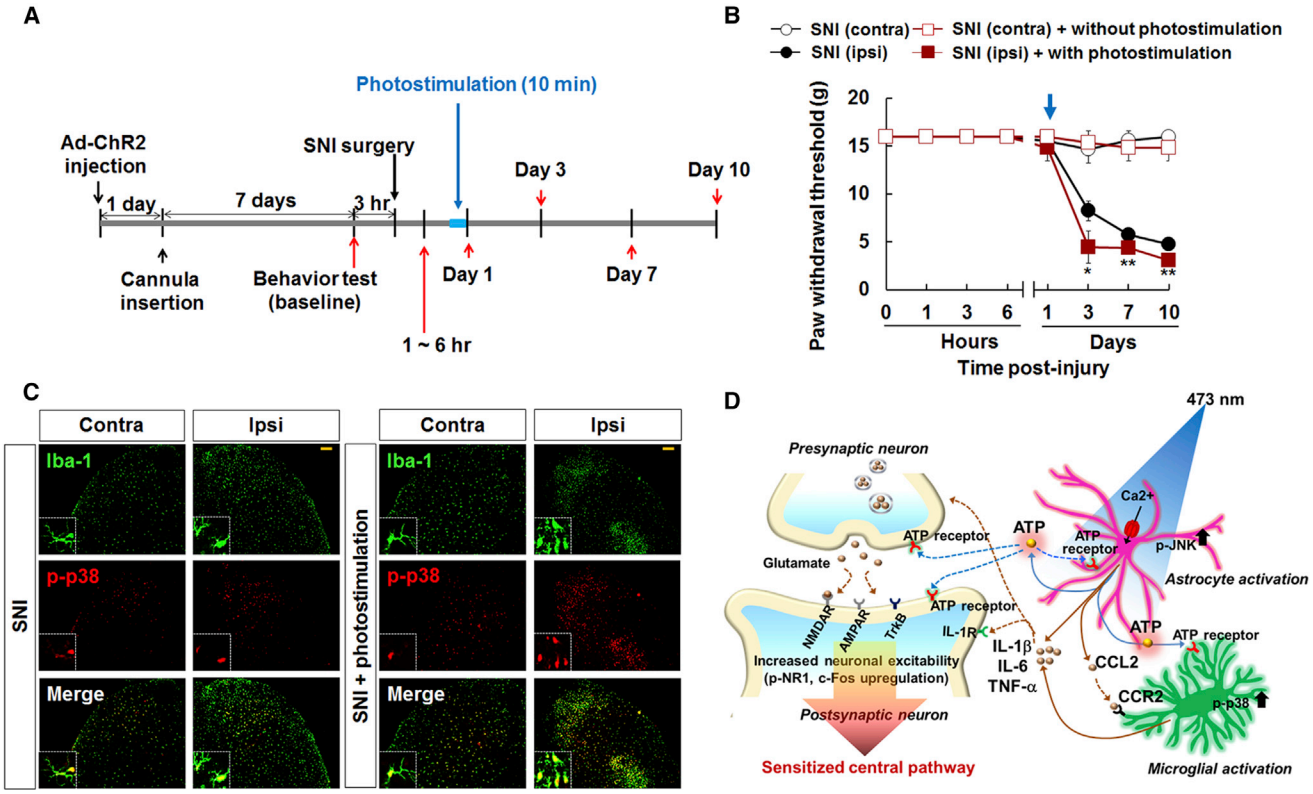

Figure 7. Optogenetic Stimulation of Spinal Astrocytes Enhances Pain Hypersensitivity in a Rat Model of Neuropathic Pain

(A) Experimental timeline of virus injection, cannula insertion, SNI surgery, photostimulation, and behavioral analysis. Seven days after Ad-ChR2 virus injection, peripheral nerve injury was induced via surgery, photostimulation was delivered for 10 min through the optogenetic fiber, and behavioral testing was completed as indicated.

(B) Rats were assessed for nociceptive responses to mechanical stimuli at baseline, 1 hr, 3 hr, 6 hr, and days 1, 3, 7, and 10 after SNI surgery and photostimulation. Blue arrows indicate the time of photostimulation. The results are expressed as mean ± SEM (n = 4–6). *p < 0.05, **p < 0.01, SNI (ipsi) versus SNI (ipsi) + with photostimulation. Data were analyzed using Mann-Whitney U tests.

(C) Frozen sections of lumbar spinal cords taken from SNI or SNI + photostimulated rats at day 1 after photostimulation were stained with anti-Iba-1 and anti-p-p38 antibodies.

(D) Proposed mechanism of pain induction following optogenetic stimulation of astrocytes in the spinal cord.

to confirm the effect of L-α-AA and SNI on microglial activation. CX3CR1 and ITGAM are expressed by microglia and play an important role in microglial activation during neuropathic pain (Clark and Malcangio, 2014; Tanga et al., 2004). After SNI surgery, the expression of *Cx3cr1* and *Itgam* mRNA was markedly increased in the ipsilateral side, which was significantly attenuated by L-α-AA injection (Figure S6D). These results suggest that astrocytic activation is required for the initiation of neuropathic pain and microglial activation.

DISCUSSION

Optogenetic techniques, which enable the selective activation of target cells within neural circuits, have accelerated the investigation of mechanisms underlying pain pathogenesis in recent years (Cai et al., 2014; Li et al., 2015). Several studies have reported an increase in behaviors associated with pain hypersensitivity following the optogenetic stimulation of ChR2-expressing neurons in the peripheral nerves and dorsal root ganglia of freely moving animals (Daou et al., 2013; Towne et al., 2013). However, pain studies employing optogenetic tools in the spinal cord have been limited so far to only neurons and ex vivo conditions (Caggiano et al., 2014; Hägglund et al., 2010; Montgomery et al., 2015; Park et al., 2015). Neuronal responses in spinal cord slices have been recorded during the selective activation of ChR2-expressing unmyelinated sensory afferents by optogenetic stimulation (Wang and Zylka, 2009). Similarly, Zhang et al. have reported an increase in the action potential and calcium channel activation following the optogenetic stimulation of ChR2-expressing neurons in spinal cord slices (Zhang et al., 2014). These findings correlate with the results of the current study and similar experiments reporting an increase in neuronal excitability following spinal astrocyte activation (Woolf and Salter, 2000). In the current study, we addressed the role of astrocytes, rather than neurons, in the dorsal horn of the spinal cord in vivo by successfully activating spinal astrocytes via the intrathecal delivery of the ChR2 adenovirus. Intrathecal injection of the ChR2 virus enabled the expression of ChR2 in dorsal horn astrocytes, which were selectively stimulated by laser illumination through a cannula implanted on the lumbar vertebra. The

localization of the cannula and optogenetic fiber enabled precise targeting of spinal astrocytes without causing damage to tissue. Herein, we report a substantial and mechanistically significant alteration in the nociceptive behaviors of freely moving animals following the direct optogenetic stimulation of dorsal horn astrocytes in the spinal cord. Our findings advocate a promising application of optogenetic tools to the spinal cord of freely moving animals in order to overcome the shortcomings of previous methodologies.

Glial activation and neuron-glial interactions are the key mechanisms underlying the pathogenesis of chronic pain (McMahon and Malcangio, 2009). Reactive astrogliosis, defined by the enhanced expression of GFAP and cellular hypertrophy, has been observed in various neuropathic and inflammatory pain conditions (Ji et al., 2013; Raghavendra et al., 2004), suggesting that astrocytes are critically involved in the pathogenesis of chronic pain (Guo et al., 2007; Ji et al., 2013). The intrathecal administration of an astrocyte toxin (Zhuang et al., 2006), glial metabolic inhibitor (Milligan et al., 2003), or JNK inhibitor (Zhuang et al., 2006) attenuates astrocyte activation and diminishes peripheral nerve-injury- and inflammation-induced pain. Moreover, transplanted astrocytes have been implicated in the induction of pain-like behaviors. Hofstetter et al. and Davies et al. have reported that astrocytes derived from neural stem cells or glial-restricted precursor cells promoted the onset of mechanical allodynia when implanted into the injured spinal cord (Davies et al., 2008; Hofstetter et al., 2005). Moreover, the intrathecal administration of TNF-α-activated astrocytes produced a persistent pain response in naive rodents via the release of MCP-1 (Gao et al., 2010b). However, the relevance of local astrocytes in the dorsal horn of the spinal cord to the production of pain pathogenesis remains to be investigated. In the current study, we have demonstrated that optogenetically stimulated spinal astrocytes can induce central pain sensitization in naive rats. Furthermore, our results suggest that the optogenetic induction of central sensitization results from the enhanced release of ATP and proalgesic mediators from activated spinal astrocytes. In the initial stage, ATP released from optogenetically stimulated astrocytes is converted to adenosine, which may initiate pain response through A1 receptor in inhibitory interneurons. Subsequently, optogenetically stimulated astrocytes may induce microglial activation and neuronal activity by releasing a variety of proalgesic mediators; these processes may account for the increased pain response in the late stage (at 1 day after the photostimulation) (Figure 7D). In the pain behaviors, the optogenetic induction of mechanical allodynia was greater than induction of thermal hyperalgesia. Our electrophysiology data suggest that ATP released from activated astrocytes after optogenetic stimulation may induce the pain hypersensitivity by inhibiting GABAergic inhibitory interneurons via A1-receptor-dependent pathway. GABAergic and glycinergic inhibitory systems have previously been associated with the development of mechanical allodynia, but not thermal hyperalgesia (Polgár et al., 2003). Combining our results with these previous reports, we speculate that thermal hyperalgesia response might be less affected, compared with mechanical allodynia, by GABAergic inhibitory system following optogenetic stimulation of spinal astrocytes. In addition, optogenetic stimulation exacerbated neuropathic pain responses induced by peripheral nerve injury, indicating a pivotal role for spinal astrocytes in the regulation of pain hypersensitivity. Such results are consistent with previous reports, suggesting a crucial role for spinal astrocytes in the pathogenesis of chronic pain. These findings enrich current knowledge, providing direct evidence for an association between pain pathogenesis and astrocyte activation, obtained via the specific in situ modulation of dorsal horn astrocytes.

We report the first known use of optogenetic techniques to stimulate spinal astrocytes in living animals, and the results provide sufficient evidence to support an astrocentric mechanism for pain pathogenesis. This suggests that the suppression of astrocyte activation might hold immense therapeutic promise for the treatment of chronic pain. The current study also provides a new experimental model for chronic pain, in which the role of spinal astrocytes in pain processing and CNS pain modulation can be identified, negating the need for nerve or tissue injury. Optogenetic stimulation provides a reversible method of modulating central sensitization within the spinal cord of freely moving animals, which could be applied to other spinal cord disease models.

EXPERIMENTAL PROCEDURES

Detailed experimental procedures are provided in Supplemental Experimental Procedures.

Subjects

All procedures in the current study were approved by the Institutional Animal Care Committee of Kyungpook National University and were performed in accordance with the animal care guidelines of the National Institutes of Health for the Care and Use of Laboratory Animals. Adult male Sprague-Dawley rats (Samtaco, Osan, Korea) weighing between 200 and 250 g were used in the described experiments. Animals were housed individually in Plexiglas cages at an ambient temperature of 23 ± 2°C and a strict 12 hr light cycle (light on from 07:00 to 19:00). Food and water were available ad libitum. Animals were allowed on average 7 days to habituate to the new environment prior to experimental onset.

Viral Injection

Following habituation, adult rats were intrathecally injected using a microperfusion pump with 10 μL of adenoviral vector expressing channelrhodopsin variant under the control of GFAP promoter (AVV-GFAP-ChR2(H134R)-Katushka1.3 (1.6×10^{11} plaque-forming units [PFU]/mL), kindly provided by Dr. Sergey Kasparov (University of Bristol, Bristol, UK) (Gourine et al., 2010) or control adenovirus expressing GFP. The adenovirus was administered at a flow rate of 0.5 μl/min. Channelrhodopsin was successfully expressed in the spinal cord dorsal horn by intrathecal delivery of adenovirus as previously described (Maeda et al., 2008; Towne et al., 2009).

Optogenetic Cannula Implantation

After 1 day post-injection, the rats were anesthetized via the intraperitoneal injection of a 2-mL/kg cocktail of 10 mL ketamine hydrochloride (50 mg/mL, Yuhan), 1.1 mL of xylazine hydrochloride (23.32 mg/mL, Bayer), and 2.67 mL of saline. After mounting the animals onto the stereotaxic apparatus (David-Kopf Instrument), the spinal cord was secured using additional clamps along the vertebrae. The skin was incised and then connective tissue and muscles were removed to expose bony structures in the lumbar spinal cord region. The dural membrane was not breached and spinal cord tissue was left untouched during the entire procedure. A dental drill was used to create a small hole without damaging the spinal cord, and a mono fiber-optic cannula (Doric Lenses) was implanted 0.5 mm below the bone surface in epidural space. The cannulae were secured in place using dental cement.

Photostimulation

Photostimulation was delivered through the optic fiber for 5, 10, or 20 min using DPSS 473-nm blue lasers (30 ms light on, 60 ms light off cycle, 20 Hz, 2.5 mW/mm^2) (Shanghai Dream Laser Technology) to ChR2-expressing spinal astrocytes.

Mechanical Sensitivity and Thermal Sensitivity

Monofilaments were used to determine the stimulus intensity threshold stiffness required to elicit hind paw withdrawal responses. Thermal pain sensitivity was assessed using the plantar test and tail immersion test.

In Vitro Optogenetic Stimulation

Astrocytes were infected with Ad-ChR2 or Ad-GFP for 48 hr. Astrocytes expressing ChR2 or GFP were illuminated for 5, 10, and 20 min with blue light at 460–475 nm using a light-emitting diode (LED) (Tu et al., 2014).

Statistical Analysis

All values are expressed as the mean ± SEM (in vivo data) or mean ± SD (in vitro data), as indicated in the figure legends. A Student's t test was used to determine the statistical significance for alterations in extracellular ATP and the percentage of microglia depletion in spinal cord tissues. Significant differences in the electrophysiology data were tested using a Student's paired two-tailed t test. All other datasets were analyzed using a one-way ANOVA with Bonferroni's post hoc tests (in vitro experiments) or one-way ANOVA with repeated-measurement (thermal hyperalgesia) or a Mann-Whitney U test (mechanical allodynia) using SPSS v.14.0 K (SPSS). Statistical significance was established at $p < 0.05$.

SUPPLEMENTAL INFORMATION

Supplemental Information includes Supplemental Experimental Procedures, six figures, and one table and can be found with this article online at http://dx.doi.org/10.1016/j.celrep.2016.11.043.

AUTHOR CONTRIBUTIONS

Y.N. designed and performed research, analyzed the data, and prepared the manuscript; Jae-Hong Kim and Jong-Heon Kim performed a part of in vitro and in vivo experiments, respectively; M.K.J. performed spared nerve injury surgery; J.Y.J. and M.-G.L. analyzed the data of motor behavioral testing. I.-S.C. and I.-S.J. performed electrophysiological studies; D.G.L., S.-H.H., and H.-J.C. contributed new reagents/analytical tools and analyzed data; and K.S. directed the study and was involved in all aspects of the experimental design, data analysis, and manuscript preparation.

ACKNOWLEDGMENTS

This work was supported by a grant from the Korea Healthcare Technology R&D Project, Ministry of Health & Welfare, Republic of Korea (HI14C331). This work was also supported by the Basic Science Research Program through the National Research Foundation (NRF) funded by the Korean Ministry of Education, Science, and Technology (MEST) (2008-0062282, 2016M3C7A1904148).

Received: March 12, 2016
Revised: October 17, 2016
Accepted: November 12, 2016
Published: December 13, 2016

REFERENCES

Airan, R.D., Thompson, K.R., Fenno, L.E., Bernstein, H., and Deisseroth, K. (2009). Temporally precise in vivo control of intracellular signalling. Nature *458*, 1025–1029.

Beppu, K., Sasaki, T., Tanaka, K.F., Yamanaka, A., Fukazawa, Y., Shigemoto, R., and Matsui, K. (2014). Optogenetic countering of glial acidosis suppresses glial glutamate release and ischemic brain damage. Neuron *81*, 314–320.

Caggiano, V., Sur, M., and Bizzi, E. (2014). Rostro-caudal inhibition of hindlimb movements in the spinal cord of mice. PLoS ONE *9*, e100865.

Cai, Y.Q., Wang, W., Hou, Y.Y., and Pan, Z.Z. (2014). Optogenetic activation of brainstem serotonergic neurons induces persistent pain sensitization. Mol. Pain *10*, 70.

Carr, F.B., and Zachariou, V. (2014). Nociception and pain: lessons from optogenetics. Front. Behav. Neurosci. *8*, 69.

Carter, M.E., Yizhar, O., Chikahisa, S., Nguyen, H., Adamantidis, A., Nishino, S., Deisseroth, K., and de Lecea, L. (2010). Tuning arousal with optogenetic modulation of locus coeruleus neurons. Nat. Neurosci. *13*, 1526–1533.

Choi, I.S., Cho, J.H., Lee, M.G., and Jang, I.S. (2015). Enzymatic conversion of ATP to adenosine contributes to ATP-induced inhibition of glutamate release in rat medullary dorsal horn neurons. Neuropharmacology *93*, 94–102.

Clark, A.K., and Malcangio, M. (2014). Fractalkine/CX3CR1 signaling during neuropathic pain. Front. Cell. Neurosci. *8*, 121.

Clark, A.K., Old, E.A., and Malcangio, M. (2013). Neuropathic pain and cytokines: current perspectives. J. Pain Res. *6*, 803–814.

Coyle, D.E. (1998). Partial peripheral nerve injury leads to activation of astroglia and microglia which parallels the development of allodynic behavior. Glia *23*, 75–83.

Daou, I., Tuttle, A.H., Longo, G., Wieskopf, J.S., Bonin, R.P., Ase, A.R., Wood, J.N., De Koninck, Y., Ribeiro-da-Silva, A., Mogil, J.S., and Séguéla, P. (2013). Remote optogenetic activation and sensitization of pain pathways in freely moving mice. J. Neurosci. *33*, 18631–18640.

Davies, J.E., Pröschel, C., Zhang, N., Noble, M., Mayer-Pröschel, M., and Davies, S.J. (2008). Transplanted astrocytes derived from BMP- or CNTF-treated glial-restricted precursors have opposite effects on recovery and allodynia after spinal cord injury. J. Biol. *7*, 24.

Duan, S., Anderson, C.M., Keung, E.C., Chen, Y., Chen, Y., and Swanson, R.A. (2003). P2X7 receptor-mediated release of excitatory amino acids from astrocytes. J. Neurosci. *23*, 1320–1328.

Gao, Y.J., and Ji, R.R. (2008). Activation of JNK pathway in persistent pain. Neurosci. Lett. *437*, 180–183.

Gao, X., Kim, H.K., Chung, J.M., and Chung, K. (2005). Enhancement of NMDA receptor phosphorylation of the spinal dorsal horn and nucleus gracilis neurons in neuropathic rats. Pain *116*, 62–72.

Gao, Y.J., Xu, Z.Z., Liu, Y.C., Wen, Y.R., Decosterd, I., and Ji, R.R. (2010a). The c-Jun N-terminal kinase 1 (JNK1) in spinal astrocytes is required for the maintenance of bilateral mechanical allodynia under a persistent inflammatory pain condition. Pain *148*, 309–319.

Gao, Y.J., Zhang, L., and Ji, R.R. (2010b). Spinal injection of TNF-α-activated astrocytes produces persistent pain symptom mechanical allodynia by releasing monocyte chemoattractant protein-1. Glia *58*, 1871–1880.

Goold, C.P., and Nicoll, R.A. (2010). Single-cell optogenetic excitation drives homeostatic synaptic depression. Neuron *68*, 512–528.

Gourine, A.V., Kasymov, V., Marina, N., Tang, F., Figueiredo, M.F., Lane, S., Teschemacher, A.G., Spyer, K.M., Deisseroth, K., and Kasparov, S. (2010). Astrocytes control breathing through pH-dependent release of ATP. Science *329*, 571–575.

Guo, W., Wang, H., Watanabe, M., Shimizu, K., Zou, S., LaGraize, S.C., Wei, F., Dubner, R., and Ren, K. (2007). Glial-cytokine-neuronal interactions underlying the mechanisms of persistent pain. J. Neurosci. *27*, 6006–6018.

Gwak, Y.S., Kang, J., Unabia, G.C., and Hulsebosch, C.E. (2012). Spatial and temporal activation of spinal glial cells: role of gliopathy in central neuropathic pain following spinal cord injury in rats. Exp. Neurol. *234*, 362–372.

Hägglund, M., Borgius, L., Dougherty, K.J., and Kiehn, O. (2010). Activation of groups of excitatory neurons in the mammalian spinal cord or hindbrain evokes locomotion. Nat. Neurosci. *13*, 246–252.

Ho, Y.C., Cheng, J.K., and Chiou, L.C. (2013). Hypofunction of glutamatergic neurotransmission in the periaqueductal gray contributes to nerve-injury-induced neuropathic pain. J. Neurosci. *33*, 7825–7836.

Hofstetter, C.P., Holmström, N.A., Lilja, J.A., Schweinhardt, P., Hao, J., Spenger, C., Wiesenfeld-Hallin, Z., Kurpad, S.N., Frisén, J., and Olson, L. (2005). Allodynia limits the usefulness of intraspinal neural stem cell grafts; directed differentiation improves outcome. Nat. Neurosci. *8*, 346–353.

Honore, P., Rogers, S.D., Schwei, M.J., Salak-Johnson, J.L., Luger, N.M., Sabino, M.C., Clohisy, D.R., and Mantyh, P.W. (2000). Murine models of inflammatory, neuropathic and cancer pain each generates a unique set of neurochemical changes in the spinal cord and sensory neurons. Neuroscience *98*, 585–598.

Illes, P., Verkhratsky, A., Burnstock, G., and Franke, H. (2012). P2X receptors and their roles in astroglia in the central and peripheral nervous system. Neuroscientist *18*, 422–438.

Iyer, S.M., Montgomery, K.L., Towne, C., Lee, S.Y., Ramakrishnan, C., Deisseroth, K., and Delp, S.L. (2014). Virally mediated optogenetic excitation and inhibition of pain in freely moving nontransgenic mice. Nat. Biotechnol. *32*, 274–278.

Ji, R.R., Berta, T., and Nedergaard, M. (2013). Glia and pain: is chronic pain a gliopathy? Pain *154* (*Suppl 1*), S10–S28.

Jiang, B.C., Cao, D.L., Zhang, X., Zhang, Z.J., He, L.N., Li, C.H., Zhang, W.W., Wu, X.B., Berta, T., Ji, R.R., and Gao, Y.J. (2016). CXCL13 drives spinal astrocyte activation and neuropathic pain via CXCR5. J. Clin. Invest. *126*, 745–761.

Li, B., Yang, X.Y., Qian, F.P., Tang, M., Ma, C., and Chiang, L.Y. (2015). A novel analgesic approach to optogenetically and specifically inhibit pain transmission using TRPV1 promoter. Brain Res. *1609*, 12–20.

Maeda, S., Kawamoto, A., Yatani, Y., Shirakawa, H., Nakagawa, T., and Kaneko, S. (2008). Gene transfer of GLT-1, a glial glutamate transporter, into the spinal cord by recombinant adenovirus attenuates inflammatory and neuropathic pain in rats. Mol. Pain *4*, 65.

Marchand, F., Perretti, M., and McMahon, S.B. (2005). Role of the immune system in chronic pain. Nat. Rev. Neurosci. *6*, 521–532.

McMahon, S.B., and Malcangio, M. (2009). Current challenges in glia-pain biology. Neuron *64*, 46–54.

Milligan, E.D., Twining, C., Chacur, M., Biedenkapp, J., O'Connor, K., Poole, S., Tracey, K., Martin, D., Maier, S.F., and Watkins, L.R. (2003). Spinal glia and proinflammatory cytokines mediate mirror-image neuropathic pain in rats. J. Neurosci. *23*, 1026–1040.

Montgomery, K.L., Yeh, A.J., Ho, J.S., Tsao, V., Mohan Iyer, S., Grosenick, L., Ferenczi, E.A., Tanabe, Y., Deisseroth, K., Delp, S.L., and Poon, A.S. (2015). Wirelessly powered, fully internal optogenetics for brain, spinal and peripheral circuits in mice. Nat. Methods *12*, 969–974.

Nagel, G., Szellas, T., Huhn, W., Kateriya, S., Adeishvili, N., Berthold, P., Ollig, D., Hegemann, P., and Bamberg, E. (2003). Channelrhodopsin-2, a directly light-gated cation-selective membrane channel. Proc. Natl. Acad. Sci. USA *100*, 13940–13945.

Park, S.I., Brenner, D.S., Shin, G., Morgan, C.D., Copits, B.A., Chung, H.U., Pullen, M.Y., Noh, K.N., Davidson, S., Oh, S.J., et al. (2015). Soft, stretchable, fully implantable miniaturized optoelectronic systems for wireless optogenetics. Nat. Biotechnol. *33*, 1280–1286.

Polgár, E., Hughes, D.I., Riddell, J.S., Maxwell, D.J., Puskár, Z., and Todd, A.J. (2003). Selective loss of spinal GABAergic or glycinergic neurons is not necessary for development of thermal hyperalgesia in the chronic constriction injury model of neuropathic pain. Pain *104*, 229–239.

Raghavendra, V., Tanga, F.Y., and DeLeo, J.A. (2004). Complete Freunds adjuvant-induced peripheral inflammation evokes glial activation and proinflammatory cytokine expression in the CNS. Eur. J. Neurosci. *20*, 467–473.

Sasaki, T., Beppu, K., Tanaka, K.F., Fukazawa, Y., Shigemoto, R., and Matsui, K. (2012). Application of an optogenetic byway for perturbing neuronal activity via glial photostimulation. Proc. Natl. Acad. Sci. USA *109*, 20720–20725.

Scholz, J., and Woolf, C.J. (2007). The neuropathic pain triad: neurons, immune cells and glia. Nat. Neurosci. *10*, 1361–1368.

Shi, Y., Gelman, B.B., Lisinicchia, J.G., and Tang, S.J. (2012). Chronic-pain-associated astrocytic reaction in the spinal cord dorsal horn of human immunodeficiency virus-infected patients. J. Neurosci. *32*, 10833–10840.

Sloan, S.A., and Barres, B.A. (2014). The detrimental role of glial acidification during ischemia. Neuron *81*, 221–223.

Street, S.E., Kramer, N.J., Walsh, P.L., Taylor-Blake, B., Yadav, M.C., King, I.F., Vihko, P., Wightman, R.M., Millán, J.L., and Zylka, M.J. (2013). Tissue-nonspecific alkaline phosphatase acts redundantly with PAP and NT5E to generate adenosine in the dorsal spinal cord. J. Neurosci. *33*, 11314–11322.

Sung, C.S., Cherng, C.H., Wen, Z.H., Chang, W.K., Huang, S.Y., Lin, S.L., Chan, K.H., and Wong, C.S. (2012). Minocycline and fluorocitrate suppress spinal nociceptive signaling in intrathecal IL-1β-induced thermal hyperalgesic rats. Glia *60*, 2004–2017.

Svensson, C.I., Marsala, M., Westerlund, A., Calcutt, N.A., Campana, W.M., Freshwater, J.D., Catalano, R., Feng, Y., Protter, A.A., Scott, B., and Yaksh, T.L. (2003). Activation of p38 mitogen-activated protein kinase in spinal microglia is a critical link in inflammation-induced spinal pain processing. J. Neurochem. *86*, 1534–1544.

Tanga, F.Y., Raghavendra, V., and DeLeo, J.A. (2004). Quantitative real-time RT-PCR assessment of spinal microglial and astrocytic activation markers in a rat model of neuropathic pain. Neurochem. Int. *45*, 397–407.

Towne, C., Pertin, M., Beggah, A.T., Aebischer, P., and Decosterd, I. (2009). Recombinant adeno-associated virus serotype 6 (rAAV2/6)-mediated gene transfer to nociceptive neurons through different routes of delivery. Mol. Pain *5*, 52.

Towne, C., Montgomery, K.L., Iyer, S.M., Deisseroth, K., and Delp, S.L. (2013). Optogenetic control of targeted peripheral axons in freely moving animals. PLoS ONE *8*, e72691.

Tsuda, M., Shigemoto-Mogami, Y., Koizumi, S., Mizokoshi, A., Kohsaka, S., Salter, M.W., and Inoue, K. (2003). P2X4 receptors induced in spinal microglia gate tactile allodynia after nerve injury. Nature *424*, 778–783.

Tsuda, M., Hasegawa, S., and Inoue, K. (2007). P2X receptors-mediated cytosolic phospholipase A2 activation in primary afferent sensory neurons contributes to neuropathic pain. J. Neurochem. *103*, 1408–1416.

Tu, J., Yang, F., Wan, J., Liu, Y., Zhang, J., Wu, B., Liu, Y., Zeng, S., and Wang, L. (2014). Light-controlled astrocytes promote human mesenchymal stem cells toward neuronal differentiation and improve the neurological deficit in stroke rats. Glia *62*, 106–121.

Wang, H., and Zylka, M.J. (2009). Mrgprd-expressing polymodal nociceptive neurons innervate most known classes of substantia gelatinosa neurons. J. Neurosci. *29*, 13202–13209.

White, J.P., Cibelli, M., Fidalgo, A.R., and Nagy, I. (2011). Extracellular signal-regulated kinases in pain of peripheral origin. Eur. J. Pharmacol. *650*, 8–17.

Woolf, C.J. (2010). What is this thing called pain? J. Clin. Invest. *120*, 3742–3744.

Woolf, C.J., and Salter, M.W. (2000). Neuronal plasticity: increasing the gain in pain. Science *288*, 1765–1769.

Zhang, H., Yoon, S.Y., Zhang, H., and Dougherty, P.M. (2012). Evidence that spinal astrocytes but not microglia contribute to the pathogenesis of Paclitaxel-induced painful neuropathy. J. Pain *13*, 293–303.

Zhang, Y., Yue, J., Ai, M., Ji, Z., Liu, Z., Cao, X., and Li, L. (2014). Channelrhodopsin-2-expressed dorsal root ganglion neurons activates calcium channel currents and increases action potential in spinal cord. Spine *39*, E865–E869.

Zhuang, Z.Y., Wen, Y.R., Zhang, D.R., Borsello, T., Bonny, C., Strichartz, G.R., Decosterd, I., and Ji, R.R. (2006). A peptide c-Jun N-terminal kinase (JNK) inhibitor blocks mechanical allodynia after spinal nerve ligation: respective roles of JNK activation in primary sensory neurons and spinal astrocytes for neuropathic pain development and maintenance. J. Neurosci. *26*, 3551–3560.

Cell Reports, Volume *17*

Supplemental Information

Reversible Induction of Pain Hypersensitivity following Optogenetic Stimulation of Spinal Astrocytes

Youngpyo Nam, Jae-Hong Kim, Jong-Heon Kim, Mithilesh Kumar Jha, Ji Young Jung, Maan-Gee Lee, In-Sun Choi, Il-Sung Jang, Dong Gun Lim, Sung-Hun Hwang, Hee-Jung Cho, and Kyoungho Suk

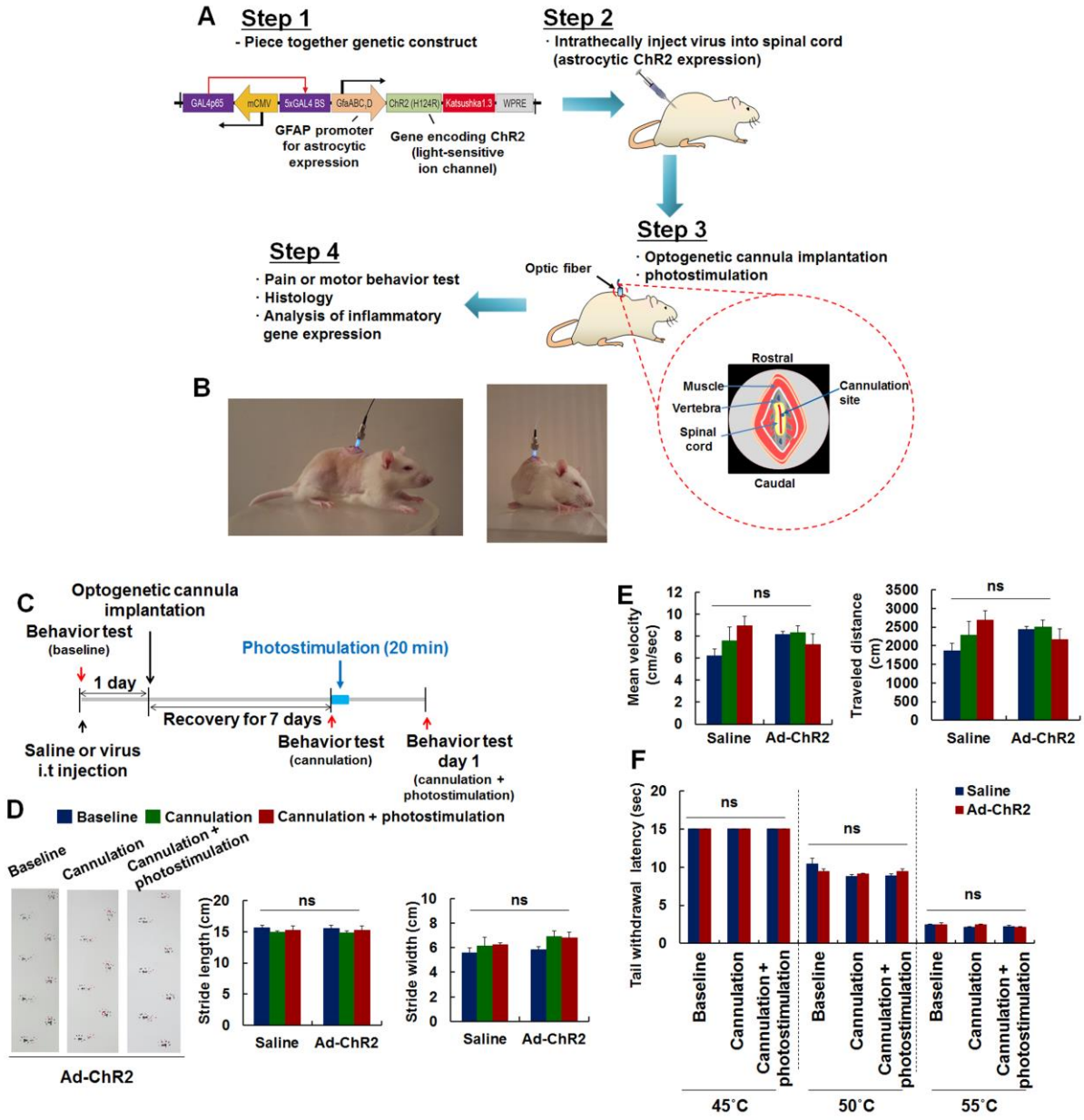

Figure S1. Related to Figure 2; Experimental procedure for the optogenetic stimulation of spinal astrocytes *in vivo* (A, B) and assessment of motor coordination and reflexive pain behavior in optogenetically stimulated rats (C-F). (**A**) The adenoviral vector expressing channelrhodopsin variant under the control of GFAP promoter (AVV-GFAP-ChR2 (H134R)-Katushka1.3) (Ad-ChR2) was used to infect spinal astrocytes [step 1]. The expression ChR2 is controlled by a shortened version of GFAP promoter, GfaABC1D.

mCMV operating in the antisense orientation drives the expression of a chimeric transcriptional activator Gal4p56 while the specificity of expression in both directions is determined by GfaABC1D. Ad-ChR2 was injected intrathecally [step 2]. After 1 day, an optogenetic cannula was stereotaxically implanted into epidural space of the vertebra of the lumbar spinal cord. Subsequently, laser illumination was delivered through the optogenetic cannula to target the dorsal horn of the spinal cord [step 3]. Rats were assessed for mechanical allodynia and thermal hyperalgesia following photostimulation. The tissue sections of the lumbar spinal cord were evaluated for glial activation, alterations in molecular signaling pathways, and inflammatory gene expression [step 4]. (**B**) Images showing optogenetic fiber implantation site in the rat spinal cord. (**C**) Experimental timeline of virus injection, cannula implantation, photostimulation, and behavioral analysis. Saline- or Ad-ChR2-injected rats were subjected to cannula implantation and photostimulation. Behavioral testing incorporated the footprint test, open-field test, and tail immersion test, which were conducted as indicated. (**D**) The stride width and length of rats after cannulation or photostimulation did not differ from those of baseline. (**E**) Total distance traveled and movement speeds were not significantly altered after cannulation or photostimulation. (**F**) Tail immersion test also demonstrated no significant differences for all the conditions tested. Results are expressed as mean ± SEM (n=3). ns, not significant. Data were analyzed using one-way ANOVA with Bonferroni’s post-hoc test.

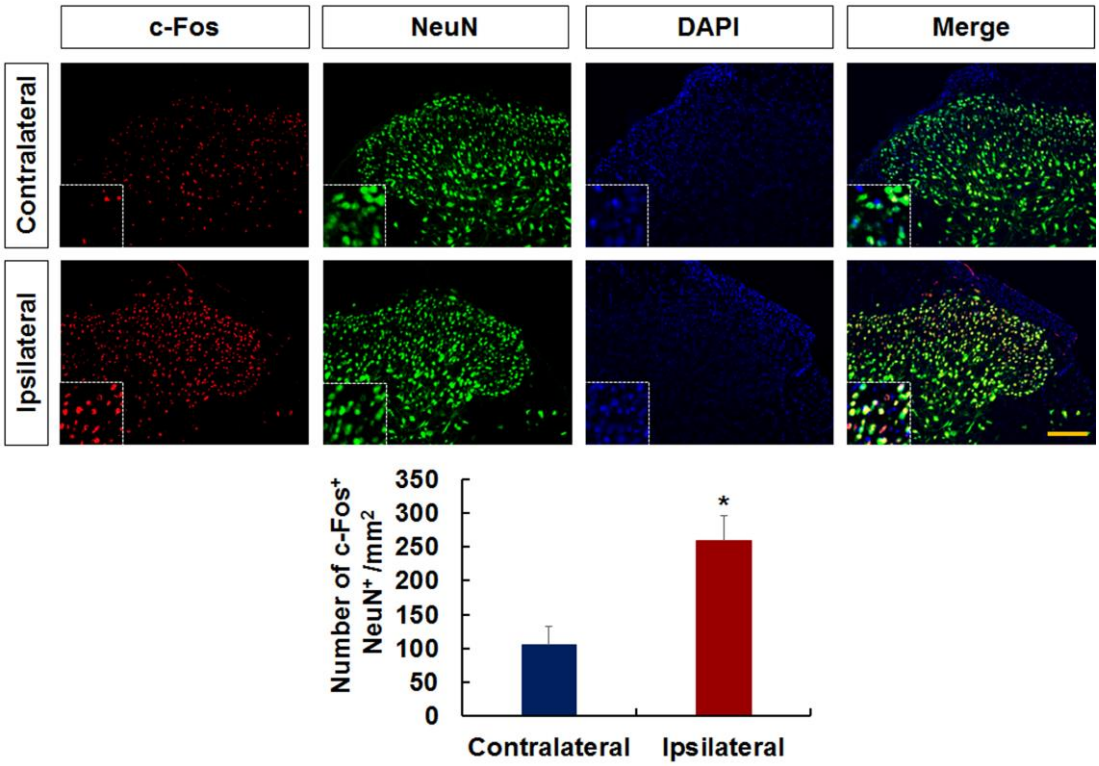

Figure S2. Related to Figure 3; Increased c-Fos immunoreactivity in the dorsal horn of the spinal cord following optogenetic stimulation. Rats were injected with Ad-ChR2 (n=4). Frozen sections of spinal cords were prepared from at day 1 post-photostimulation. Neuronal expression of c-Fos was identified in the lumbar spinal cord using anti-c-Fos and anti-NeuN antibodies. Cell nuclei were stained with DAPI to confirm the nuclear expression of c-Fos. Scale bar, 200 μm. The graph displays the quantification of c-Fos$^+$ neurons. Results are expressed as mean ± SD (n=4). *P < 0.05, contra vs. ipsi (Student's t test).

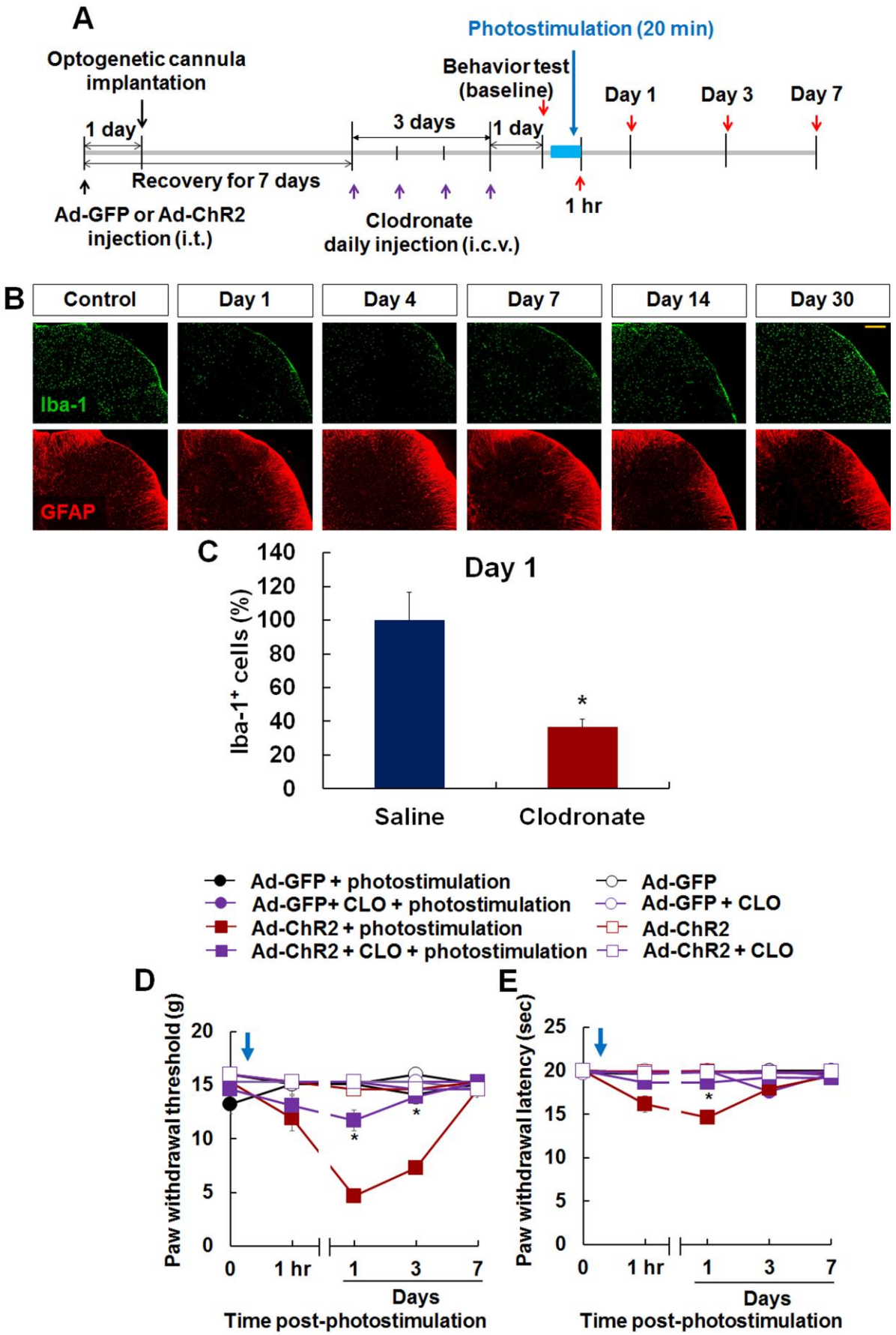
A
Photostimulation (20 min)
Optogenetic cannula implantation
Behavior test (baseline)
Day 1
Day 3
Day 7
1 day
3 days
1 day
Recovery for 7 days
Ad-GFP or Ad-ChR2 injection (i.t.)
Clodronate daily injection (i.c.v.)
1 hr
B
Control
Day 1
Day 4
Day 7
Day 14
Day 30
Iba-1
GFAP
C
Day 1
Iba-1+ cells (%)
140
120
100
80
60
40
20
0
*
Saline
Clodronate
Ad-GFP + photostimulation
Ad-GFP+ CLO + photostimulation
Ad-ChR2 + photostimulation
Ad-ChR2 + CLO + photostimulation
Ad-GFP
Ad-GFP + CLO
Ad-ChR2
Ad-ChR2 + CLO
D
Paw withdrawal threshold (g)
20
15
10
5
0
*
*
0
1 hr
1
3
7
Days
Time post-photostimulation
E
Paw withdrawal latency (sec)
25
20
15
10
5
0
*
0
1 hr
1
3
7
Days
Time post-photostimulation

Figure S3. Related to Figure 3; Microglia depletion alleviates optogenetically induced pain hypersensitivity. (**A**) Experimental timeline of virus injection, optogenetic cannula implantation, clodronate injection, photostimulation, and behavioral analysis. Seven days post-viral injection, clodronate liposome (CLO; 1.34 mg per kg body weight) or saline was injected daily via the intracerebroventricular route for 4 days (as indicated by purple arrows). (**B**) Frozen sections of the spinal cord were prepared on day 1, 4, 7, 14, and 30 post-clodronate or saline injection, and stained with the anti-Iba-1 and anti-GFAP antibodies for immunofluorescence analysis. Scale bar, 200 μm. Results are representative of more than three independent experiments. (**C**) The graph demonstrates the number of Iba-1-positive cells (%) at day 1. Results are expressed as mean ± SD (n=3). *$P < 0.05$, saline vs. clodronate (Student's *t* test). Rats then underwent photostimulation (indicated by blue arrows), followed by behavioral testing (indicated by red arrows). (**D**, **E**) Injection of clodronate decreased both mechanical and thermal pain responses after photostimulation. Blue arrows indicate the time points of photostimulation. The results are expressed as mean ± SEM (n=4). *$P < 0.05$, Ad-ChR2 + photostimulation vs. Ad-ChR2 + CLO + photostimulation. Data were analyzed using one-way ANOVA with repeated measurement (paw withdrawal latency) or Mann Whitney U tests (paw withdrawal threshold).

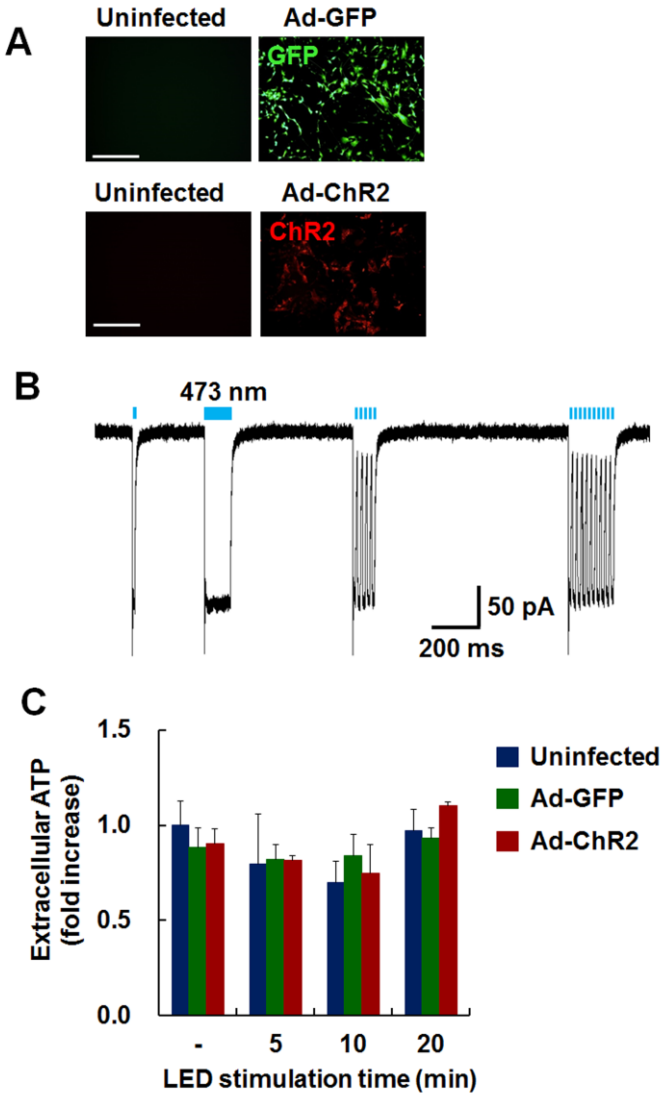

Figure S4. Related to Figure 5; Measurement of membrane current and ATP release from optogenetically stimulated primary astrocytes *in vitro*. (**A**) Primary astrocyte cultures were infected with Ad-GFP or Ad-ChR2. Scale bar, 200 μm. (**B**) ChR2 expressing astrocytes were voltage-clamped at a holding potential of -60 mV using a whole-cell patch clamp, and membrane current of astrocytes was measured in various stimulation conditions. (**C**) Infected astrocytes were illuminated using the LED device for 5, 10, or 20 min and culture media were collected 6 hr after photostimulation. ATP in the culture media was measured using a bioluminescence assay. Results are expressed as mean ± SD (n=4).

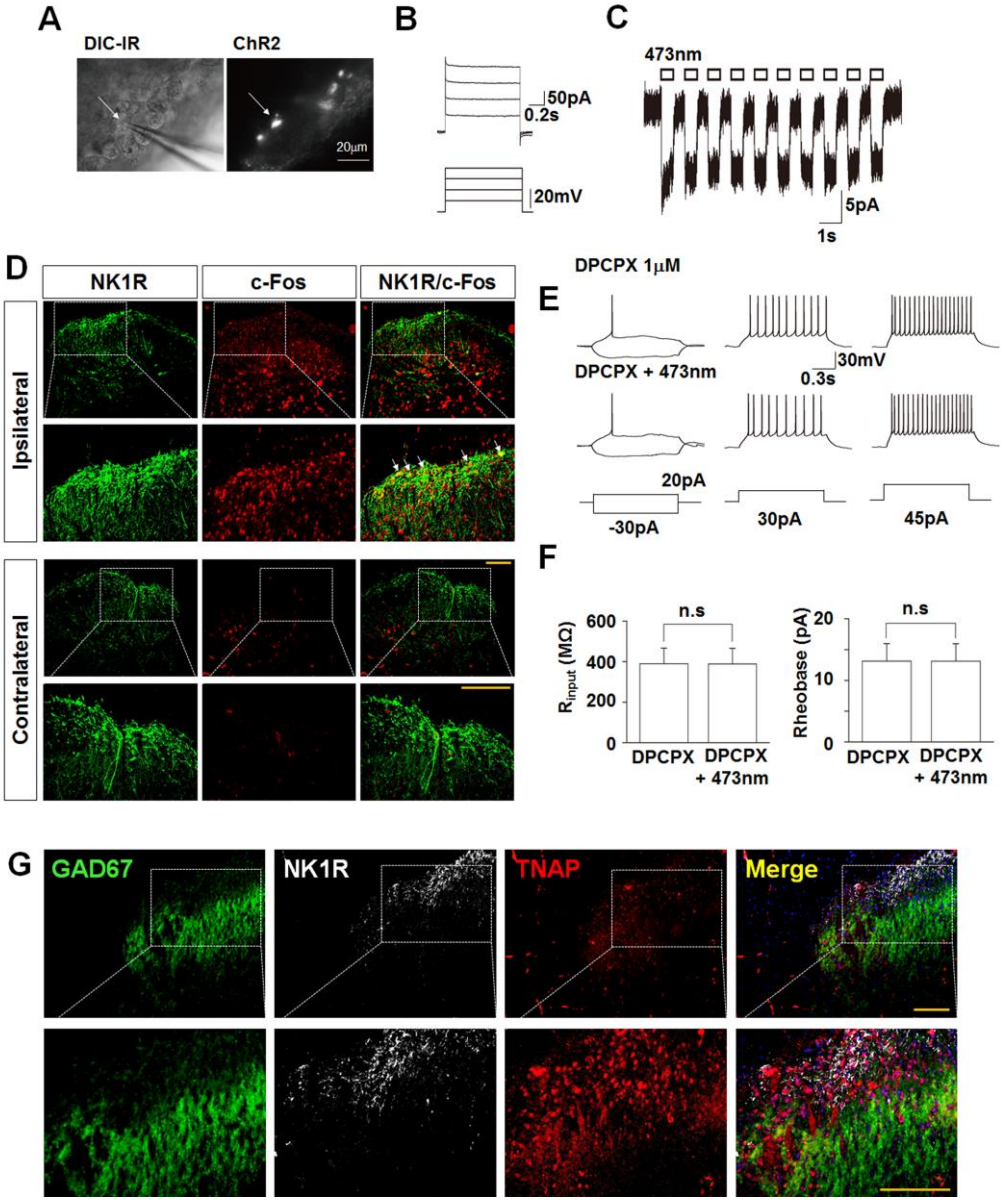

Figure S5. Related to Figure 6; Optogenetic stimulation of astrocytes in spinal cord increases c-Fos expression in projection neurons without affecting the passive membrane properties of spinal dorsal horn neurons. (A) The spinal cord was dissected and horizontally sliced at a thickness of 400 μm in a cold artificial cerebrospinal fluid, and the spinal dorsal horn region was infected with Ad-ChR2. Two days after virus infection, DIC-IR and fluorescent images of the spinal dorsal horn region in slice cultures are shown.

(**B, C**) Astrocytes expressing ChR2-Kat1.3 (arrow) were voltage-clamped at a holding potential of -80 mV. A typical trace of current responses to depolarizing step pulses (-80 mV to -40 mV, 10 mV increment) is shown (**B**). Note that depolarizing step pulses did not evoke action currents. Typical current responses to photostimulation (473 nm, 500 ms duration) are shown (**C**). Note that the photostimulation-induced inward currents were similar to those recorded from primary astrocytes expressing ChR2-Kat1.3 (see Figure S4). (**D**) Ad-ChR2-injected animals were photostimulated for 20 min. Frozen sections of spinal cord were prepared at day 1. Expression of c-Fos in projection neurons was identified in lamina I within lumbar dorsal horn using anti-c-Fos and anti-NK1R antibodies. Arrows indicate the co-localization of NK1R and c-Fos. Scale bar, 200 μm. (**E**) Typical traces of voltage responses to hyperpolarizing and depolarizing current injections before and after photostimulation (473 nm, 500 ms duration, 1 Hz) in the presence of 1 μM DPCPX. (**F**) Photostimulation-induced changes in the input resistance (Rinput, *left*) and rheobase (*right*) in the presence of 1 μM DPCPX. Each column and error bars indicate the mean and SEM from 8 experiments. n.s; not significant. The results suggest that photostimulation does not affect the membrane properties of dorsal horn neurons. Also, it should be noted that photostimulation induced inwardly directed membrane currents in astrocytes, but not in dorsal horn neurons. (**G**) Spinal cord sections from rats at 1 day after laser stimulation were evaluated for NK1R (white), TNAP (red), and GAD67 (green) expression by immunofluorescence analysis. NK1R and GAD67 expression was detected in lamina I and II regions of the spinal cord dorsal horn, respectively. Nuclei were stained with DAPI (blue). TNAP protein was co-localized with GAD67, but not NK1R, in the spinal cord dorsal horn. Scale bars, 200 μm. Results are representative of more than three independent experiments.

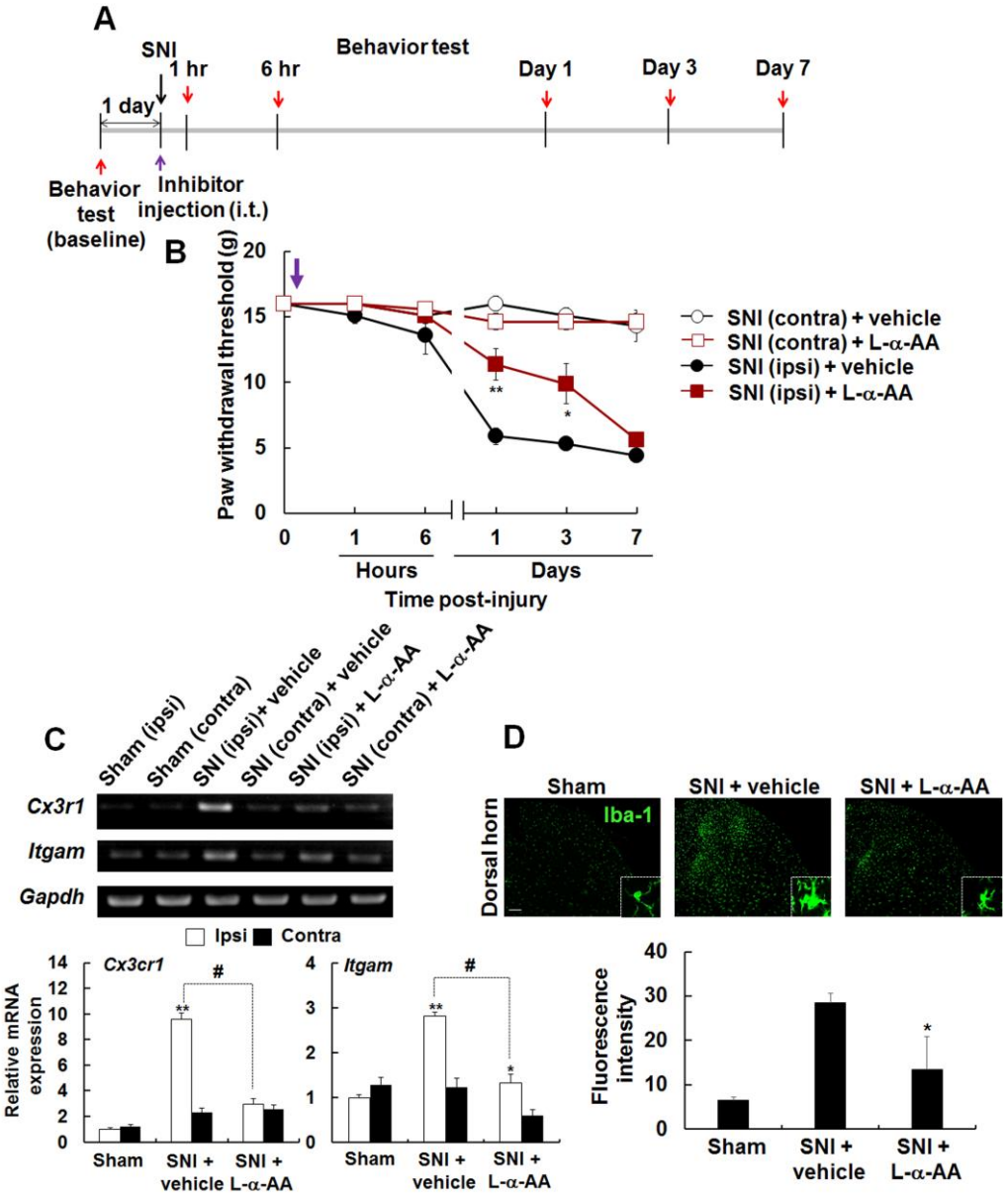

Figure S6. Related to Figure 7; Early administration of L-a-AA inhibits the development of pain response and microglial activation in SNI model. (**A**) Experimental timeline of SNI surgery, glial inhibitor injection, and behavioral analysis. Animals were injected intrathecally with L-α-AA (10 nM) or vehicle immediately after SNI surgery. (**B**) Early injection of L-α-AA reduced SNI-induced mechanical pain responses. A purple arrow indicates the time point of L-α-AA injection. Results are expressed as mean ± SEM (n=6). **P*

< 0.05, SNI (ipsi) + vehicle vs. SNI (ipsi) + L-α-AA. Data were analyzed using Mann Whitney U tests. (**C**) At day 1 following SNI surgery and inhibitor injection, total mRNA was extracted from the lumbar spinal cord of each group, and subjected to RT-PCR to assess the expression levels of *Cx3r1* and *Itgam. Gapdh* was used as an internal control. The graph displays quantitative results normalized to *Gapdh*; results are expressed as mean ± SD (n=3). **P* < 0.05, ***P* < 0.01 vs. contralateral side; $^{\#}P$ < 0.05 between the indicated groups (one-way ANOVA with Bonferroni's post-hoc test). (**D**) Spinal cord tissue sections were stained with anti-Iba-1 antibody for the assessment of microglial activation. Microglial activation was markedly decreased by L-α-AA injection, when compared with vehicle control. Scale bar, 200 μm. The graph displays quantification of fluorescence intensity. Results are expressed as mean ± SD (n=3). **P* < 0.05 vs. SNI + vehicle (Student's *t* test).

Table S1. Related to Figure 3, 6 and S6; DNA sequences of the primers used for RT-PCR.

Genes	**GenBank Accession No.**	**Primer sequences**
Cytokines		
Tnf	NM_012675	Forward : 5’- GTAGCCCACGTCGTAGCAAA -3’
		Reverse : 5’- CCCTTCTCCAGCTGGGAGAC -3’
Il1b	NM_031512	Forward : 5’- TGACTCGTGGGATGATGACG -3’
		Reverse : 5’- CTGGAGACTGCCCATTCTCG -3’
Il6	NM_012589	Forward : 5’- AAAATCTGCTCTGGTCTTCTG G -3
		Reverse : 5’- GGTTTGCCGAGTAGACCTCA -3’
Chemokine		
Ccl2	NM_021866	Forward : 5’- CTGCCCCTACTTGTCATGGT -3’
		Reverse : 5’- TGCAGAGATTTTTGGCAATG -3’
Receptor		
Cx3cr1	NM_133534	Forward : 5′ - CAGCATCGACCGGTACCT -3’
		Reverse : 5′ - CCCTCTTCATGCCACAACT -3’
Itgam	NM_012711	Forward : 5’ - CAGATCAACAAGGTGACCATATGG -3’
		Reverse : 5′ - ACAGGATTGTGAACTGTATATGGC -3’
Housekeeping gene		
Gapdh	NM_017008	Forward : 5'-ACCACAGTCCATGCCATCAC-3'
		Reverse : 5'-TCCACCACCCTGTTGCTGTA-3'

Supplemental Experimental Procedures:

Subjects

All procedures in the current study were approved by the Institutional Animal Care Committee of Kyungpook National University and were performed in accordance with the animal care guidelines of the National Institutes of Health for the Care and Use of Laboratory Animals. Adult male Sprague-Dawley rats (Samtaco, Osan, Korea) weighing between 200 and 250 g were used in the described experiments. Animals were housed individually in Plexiglas cages at an ambient temperature of 23 ± 2°C and a strict 12 hr light cycle (light on from 07:00 to 19:00). Food and water were available ad libitum. Animals were allowed on average 7 days to habituate to the new environment prior to experimental onset.

Surgical Procedures

Microdialysis

For cannula implantation, two holes were created 1 mm apart in the lumbar vertebrae using a dental drill. Two cannulas, one for optogenetic stimulation and the other for microdialysis, were implanted stereotaxically. The cannula for optogenetic stimulation was inserted obliquely, whereas the microdialysis probe cannula was inserted perpendicularly into the spinal cord dorsal horn. Following cannula implantation, the rats were housed individually and allowed to recover for 7 days. The microdialysis probe (CMA Microdialysis AB, Stockholm, Sweden) was inserted into the dorsal horn through the probe cannula 24 hr before the start of the microdialysis. Rats were maintained under isoflurane (1.5%) anesthesia and mounted onto a stereotaxic frame. The probe was connected to a microperfusion pump with polyethylene tubing and perfused with artificial cerebrospinal fluid at a flow rate of 0.5

μl/min. Extracellular fluid from the outlet end of the tube was collected in plastic vials standing in ice. Samples were collected for 2 hr over a 1-hr interval. The second dialysate was used for the measurement of ATP.

Spared Nerve Injury Induction

To create the peripheral nerve injury-induced neuropathic pain model, surgery was performed on the left side of the spine (ipsilateral to cannula implantation) in rats anaesthetized with 2% isoflurane. The three peripheral branches (the sural, common peroneal and tibial nerves) of the sciatic nerve were exposed. The common peroneal and tibial nerves were then tightly ligated with 6-0 silk thread, and a 2 mm segment of the two nerves was removed as previously described (Decosterd and Woolf, 2000). Following surgery, all wounds were irrigated with sterile saline and closed in layers. Non-operated animals were used as naive controls. The day of surgery was set as day 0.

Behavioral Analysis

Mechanical Sensitivity

Rats were habituated to the experimental room for at least 1 hr prior to behavioral testing, which was performed by two investigators. To evaluate mechanical sensitivity, rats were placed under a transparent plastic box on a metal mesh floor, where a logarithmic series of calibrated Semmes-Weinstein monofilaments (Stoelting Co., Wood Dale, IL) were applied to the left and right hind paws. Monofilaments were used to determine the stimulus intensity threshold stiffness required to elicit hind paw withdrawal responses. The 50% paw withdrawal threshold was assessed using the Dixon's up-and-down method (Chaplan et al., 1994).

Thermal Sensitivity

Thermal pain sensitivity was assessed using the plantar test and tail immersion test. Rats were placed in an acrylic box with a glass panel floor. The plantar surface of the hind paw was exposed to a beam of infrared radiant heat using the Plantar Test Analgesy-Meter (Ugo Basile, Comerio, Italy). Paw withdrawal latencies were recorded at an infrared intensity of 70 and were measured three times per session, separated by a minimum interval of 10 min. Maximum cut-offs were assigned at 20 sec. Alterations in pain sensitivity were determined by stimulating the left and right hind paws following optogenetic stimulation. For the tail immersion test, the animals were immobilized in the tube while assessment took place. The tail was immersed into a water bath at 45, 50, or 55°C. The tail withdrawal latency as indicated by hard tail movement was calculated by averaging three individual measurements. A cutoff time of 15 sec was established to prevent tissue damage.

Locomotor analysis

For footprint analysis, the fore and hind paws were coated with red- and black-colored nontoxic paint. Rats were encouraged to walk in a straight line along an 80 cm enclosed runway over white paper. Footprint patterns were then digitalized and analyzed with Photoshop software to assess motor coordination. Coordination was measured as the average distance between each stride over the duration of movement. Stride width was measured as the average distance between left and right footprints. The Open-field test was conducted as previously described with minor modifications (Jang et al., 2013). Rats were placed at the corner of the arena (60×60×45 cm; with black acrylic walls). After a 1 min habituation period, locomotor behavior was recorded for 5 min using a digital camera fixed 2 m above the floor.

Total distance traveled (cm) and movement speed (cm/sec) were analyzed using a video-tracking system (Panlab SMART video-tracking system, Barcelona, Spain). The arena was cleaned between trials with 70% ethyl alcohol. Tests were performed under a low-illumination red light.

Histological Analysis

Histological analysis was performed as previously described (Ock et al., 2010). For the immunofluorescence analysis of glial activation and neuronal excitability, tissue sections were incubated with mouse anti-GFAP (glial fibrillary acidic protein) antibody (1:500 dilution; BD Biosciences, Heidelberg, Germany), rabbit anti-Iba-1 (ionized calcium binding adaptor molecule 1) antibody (1:500 dilution; WAKO, Osaka, Japan), mouse anti-NeuN antibody (1:200 dilution; Millipore, Billerica, MA), rabbit anti-p-JNK (1:500 dilution; Cell Signaling Technology, Beverly, MA), rabbit anti-p-p38 (1:500 dilution; Cell Signaling Technology), rabbit anti-p-NR1 Ser896 (1:500 dilution; Millipore), rabbit anti-c-Fos (1:500 dilution; Abcam, Cambridge, MA), mouse anti-c-Fos (1:200 dilution; Santa Cruz Biotechnology, Santa Cruz, CA) mouse anti-GAD67 (1:200 dilution; Millipore), rabbit anti-NK1R (1:200 dilution; Sigma) and goat anti-TNAP (1:200 dilution; Abcam). Sections were visualized via incubation with FITC-conjugated anti-mouse, rat, rabbit, or goat IgG antibody, Cy5-conjugated rabbit IgG antibody and Cy3-conjugated anti-rabbit or goat IgG antibody (The Jackson Laboratory, Bar Harbor, ME). Images were captured using a CCD color video camera (Olympus D70) attached to a microscope (Olympus BX51) equipped with 50, 100, and 200x objective lens. See the Supplemental Experimental procedures for details of histological data quantification.

Quantification of histological data

For the quantification of ChR2 expression, glial activation, and neuronal excitability, three lumbar sections were examined for each animal. Adobe Photoshop software was used to indicate outline of dorsal horn area excluding edge effects and dural expression from quantification. Fluorescence intensities and the number of c-Fos-positive neurons were quantified using Image J software. Pictures were taken from five non-overlapping fields of view chosen at random for each experiment. All evaluation of ChR2 expression in dorsal horn of spinal cord were carried out in a blind fashion, and threshold for eliminating animals was based on less than 5% of GFAP+ChR2+ cells from total GFAP+ cells in spinal dorsal horn. For quantitative analysis, tissue sections from experimental groups were selected randomly. The co-localization analyses were performed as described previously (Vanlandingham and Ceresa, 2009). To quantify the co-localizations, five non-overlapping fields of view (200 μm x 200 μm) of spinal cords were selected randomly as regions of interest, and a binary image of co-localized pixels from two separate channels (GFAP/ChR2) was generated on each field using Image J software. The co-localization plug-in Image J software was also used to automate channel threshold, and co-localization was established for pixels whose intensities were higher than threshold and for which the ratio of intensity was greater than 50%. These results were presented as the ratio of fluorescence intensities of two images (ChR2/GFAP-double-positive area per total GFAP-positive area) (%).

In Vitro Optogenetic Stimulation

Neonatal astrocyte cultures were prepared from mixed glial cultures, as previously described with minor modifications (Lee et al., 2009). Primary astrocytes were obtained by

shaking mixed glial cultures at 250 rpm overnight. Culture media were discarded, and astrocytes were dissociated using trypsin-EDTA (Gibco-BRL). Astrocytes were then collected by centrifuging at 1,200 rpm for 10 min. Astrocytes were cultured at a density of 2 x 105 cells per well in 6-well plates in DMEM medium supplemented with 10% FBS and 100 U/ml penicillin-streptomycin. Astrocytes Cells were infected with Ad-ChR2 or Ad-GFP for 48 hr. Astrocytes expressing ChR2 or GFP were illuminated for 5, 10, 20 min with blue light at 460-475 nm using a light-emitting diode (LED) (Tu et al., 2014). At either 6 hr or immediately after photostimulation, total RNA or culture media were subjected to RT-PCR analysis, ELISA, or bioluminescence assay to measure the levels of proinflammatory cytokines, chemokines, and extracellular ATP.

Reverse Transcription-PCR

Total RNA was extracted from cells or tissues using TRIzol reagent (Invitrogen) according to the manufacturer's instructions. Reverse transcription was conducted using Superscript II (Invitrogen) and oligo (dT) primers. PCR amplification was achieved using a DNA Engine Tetrad Peltier Thermal Cycler (MJ Research, Waltham, MA) at an annealing temperature of 55–60°C for 20–30 cycles using specific primer sets (**Table S1**). To analyze PCR products, 10 μl of each PCR product underwent electrophoresis on 1% agarose gel and exposed to UV light following ethidium bromide staining. *Gapdh* was used as an internal control.

ELISA

The levels of TNF-α protein in the culture media were evaluated via sandwich ELISA using the rat monoclonal anti-mouse TNF-α antibody (capture antibody) and goat

biotinylated polyclonal anti-mouse TNF-α antibody (detection antibody) (ELISA development reagent; R&D Systems) as previously described (Zheng et al., 2008). The recombinant mouse TNF-α protein (R&D Systems) was used as a standard.

Cytotoxicity analysis

Cell viability was assessed using a modified 3-(4,5-dimethylthiazol-2-yl)-2,5-diphenyltetrazolium bromide (MTT) assay as previously described (Ock et al., 2010). Following LED illumination, the culture medium was aspirated and MTT (0.5 mg/mL in PBS) was added to cells. Cells were then incubated at 37°C for 3 hr. The resulting formazan crystals were dissolved in DMSO. Absorbance was determined at 570 nm using a microplate reader.

Bioluminescence assay

The extracellular ATP content of the samples was determined using an ATP bioluminescence assay kit (Sigma, St. Louis, MO) and a Synergy 4 Multi-Detection Microplate Reader (BioTek Instruments Inc., Winooski, VT). Undiluted samples (100 μl) of the culture medium from primary astrocytes or diluted samples of spinal cord dialysate (25 μl of the dialysate from the buffer-perfused spinal cord tissue mixed with 75 μl of ultrapure water) were pipetted into a 96-well microplate for ATP analysis. ATP assay mix solution (100 μl) was added to each well and the luminescence signal was assessed kinetically within 1 min.

Administration of glial inhibitors and DPCPX

L-alpha-aminoadipate (L-α-AA) (Sigma) and DL-fluorocitric acid barium salt (fluorocitrate) (Sigma) were used to inhibit astrocytic activation. L-α-AA was dissolved in

0.01 M PBS (final concentration 10 nM). Fluorocitrate was dissolved initially in 2 M HCl and then diluted in 0.01 M PBS to make a final concentration of 1 nM. A selective adenosine A1 receptor antagonist DPCPX was used to inhibit adenosine receptor. DPCPX was dissolved initially in DMSO and then diluted in saline. L-α-AA (10 μl) or fluorocitrate (10 μl) or DPCPX (5 μg/10 μl) was administrated intrathecally at a flow rate of 1 μl/min to rats

Microglial depletion

To eliminate spinal microglia, liposomal clodronate was injected as previously described with slight modifications (Jang et al., 2013; Lee et al., 2012). Rats were administered with clodronate liposome daily for 4 days (Formumax, Palo Alto, CA) (1.34 mg per kg body weight; 50 μl/rat, i.c.v. at a flow rate of 1 μl/min). To evaluate the effects of clodronate liposome administration, spinal cord sections were stained with the anti-Iba-1 antibody, and the number of Iba-1-positive microglial cells was counted using Image J software. Three slides per animal were examined.

Electrophysiology

Organotypic slice culture.

Sprague Dawley rats (3–5 d old, either sex) were decapitated under ketamine anesthesia (100 mg/kg, i. p.). The spinal cord was dissected and horizontally sliced at a thickness of 400 μm by use of a microslicer (VT1000S; Leica, Nussloch, Germany) in a cold artificial cerebrospinal fluid (aCSF; 120 NaCl, 2 KCl, 1 KH_2PO_4, 26 $NaHCO_3$, 2 $CaCl_2$, 1 $MgCl_2$ and 10 glucose, saturated with 95% O_2 and 5% CO_2). The spinal slices (L4-L6) containing the dorsal horn region were placed onto a 30-mm diameter membrane insert

(Millicell-CM, Millipore, Billerica, MA) and inserts were transferred to 6-well culture plates containing 1 ml of culture medium per well. And then, the viral vector was carefully administered onto the spinal dorsal horn region. Culture medium consisted of 50% minimum essential medium, 25% Hank's Balanced Salt Solution, 25% Heat Inactivated Horse Serum, and 1 mM glutamine (all from Sigma). The medium was supplemented with glucose to achieve the final glucose concentration of 10 mM. Slice cultures were maintained at 37°C, 5% CO_2 and humidity 100% for 2–3 days before experiments were performed.

Whole-cell patch clamp recording.

All electrical measurements were performed by use of a computer-controlled patch clamp amplifier (Axopatch 200B; Molecular Devices; Union City, CA). For whole-cell recording, patch pipettes were made from borosilicate capillary glass (1.5 mm outer diameter, 0.9 mm inner diameter; G-1.5; Narishige, Tokyo, Japan) by use of a pipette puller (P-97; Sutter Instrument Co., Novato, CA). The resistance of the recording pipettes filled with internal solution (in mM; 140 K-methanesulfonate, 10 KCl, 2 EGTA, 2 Mg-ATP and 10 HEPES, pH 7.2 with Tris-base) was 2-5 MΩ. The liquid junction potential (~ –11 mV, measured by exchanging bath solution from internal solution to standard external solution) was corrected. The pipette capacitance and series resistance were compensated for (50–70%). In current-clamp recordings, the amplifier was switched to the current-clamp (I-CLAMP) mode, and then the series resistance compensation was activated. This allowed us to provide the equivalent of 'bridge balance' in other amplifiers. The resting membrane potential was immediately measured after making the whole-cell configuration. Voltage or current was low-pass filtered at 5 kHz and acquired at 20 kHz (Digidata 1440; Molecular Devices). All experiments were performed at room temperature (22–24ºC). The bath was perfused with

aCSF at 2 ml/min by the use of a peristaltic pump (MP-1000, EYELA, Tokyo, Japan). The frequency of action potentials during the control (5 min) and photostimulation periods (5 min) was calculated for each condition. The effect of photostimulation was quantified as a percentage decrease in action potential frequency compared to the control value. Numerical values are provided as the mean ± SEM using values normalized to the control. Significant differences in action potential frequency during photostimulation were tested using Student's paired two-tailed t-test, using absolute values rather than normalized ones. Values of $p < 0.05$ were considered significantly different.

Single-cell RT-PCR.

After patch-clamp recording, the contents of recorded neuron including mRNAs were aspirated by applying a gentle suction through the recording pipette. Then the harvested material in the patch pipette was expelled into a PCR tube, and reverse transcription and 1st PCR reactions were performed in the same tube using a one-step RT-PCR kit (Qiagen, Hilden, Germany). Primers used for RT-PCR or PCR were as follows: VIAAT (inhibitory neuronal marker) (1st) 5'-gcatgttcgtgctgggtctac-3'/5'-gaacttcaccttctcccaggc-3' (2nd) 5'-gctacctggggttgttcctca-3'/5'-atggaccaggacttctgcgac-3' (product size: 301 bp), and VGluT2 (excitatory neuronal marker) (1st) 5'-cagatctacagggtgctggag-3'/5'-tctggctgcagatgggatcag-3' (2nd) 5'-atgcgactgtacgtgcttcgg-3'/5'-gatgtatccgcccggaatctg-3' (product size: 259 bp). The 2nd PCR was performed using GoTaq® DNA polymerase (Promega, Madison, WI) and each first PCR product was used as a template (2 μl).

Sample size calculation

The proper group sizes were estimated using power calculation based on effect sizes

(Faul et al., 2009; Iyer et al., 2014).

References

Chaplan, S.R., Bach, F.W., Pogrel, J.W., Chung, J.M., and Yaksh, T.L. (1994). Quantitative assessment of tactile allodynia in the rat paw. J. Neurosci. Methods *53*, 55-63.

Decosterd, I., and Woolf, C.J. (2000). Spared nerve injury: an animal model of persistent peripheral neuropathic pain. Pain *87*, 149-158.

Faul, F., Erdfelder, E., Buchner, A., and Lang, A.G. (2009). Statistical power analyses using G*Power 3.1: tests for correlation and regression analyses. Behav. Res. Methods *41*, 1149-1160.

Iyer, S.M., Montgomery, K.L., Towne, C., Lee, S.Y., Ramakrishnan, C., Deisseroth, K., and Delp, S.L. (2014). Virally mediated optogenetic excitation and inhibition of pain in freely moving nontransgenic mice. Nat. Biotechnol. *32*, 274-278.

Jang, E., Kim, J.H., Lee, S., Seo, J.W., Jin, M., Lee, M.G., Jang, I.S., Lee, W.H., and Suk, K. (2013). Phenotypic polarization of activated astrocytes: the critical role of lipocalin-2 in the classical inflammatory activation of astrocytes. J. Immunol. *191*, 5204-5219.

Lee, J.C., Seong, J., Kim, S.H., Lee, S.J., Cho, Y.J., An, J., Nam, D.H., Joo, K.M., and Cha, C.I. (2012). Replacement of microglial cells using Clodronate liposome and bone marrow transplantation in the central nervous system of SOD1(G93A) transgenic mice as an in vivo model of amyotrophic lateral sclerosis. Biochem. Biophys. Res. Commun. *418*, 359-365.

Ock, J., Han, H.S., Hong, S.H., Lee, S.Y., Han, Y.M., Kwon, B.M., and Suk, K. (2010). Obovatol attenuates microglia-mediated neuroinflammation by modulating redox regulation.

Br. J. Pharmacol. *159*, 1646-1662.

Vanlandingham, P.A., and Ceresa, B.P. (2009). Rab7 regulates late endocytic trafficking downstream of multivesicular body biogenesis and cargo sequestration. J. Biol. Chem. *284*, 12110-12124.

Zheng, L.T., Ryu, G.M., Kwon, B.M., Lee, W.H., and Suk, K. (2008). Anti-inflammatory effects of catechols in lipopolysaccharide-stimulated microglia cells: inhibition of microglial neurotoxicity. Eur. J. Pharmacol. *588*, 106-113.